





## 22 Abstract

23 Using archival research methods, we found and combined data from multiple sources to produce  
24 a unique, 140 year record of daily water temperature ( $T_w$ ) in the lower Willamette River, Oregon  
25 (1881– 1890, 1941– present). Additional daily weather and river flow records from the 1850s on-  
26 wards are used to develop and validate a statistical regression model of  $T_w$  for 1850– 2020. The  
27 model simulates the time-lagged response of  $T_w$  to air temperature and river flow, and is cali-  
28 brated for three distinct time periods: the late 19th, mid 20th, and early 21st centuries. Results  
29 show that  $T_w$  has trended upwards at  $\sim 1.1$  °C /century since the mid-19th century, with the largest  
30 shift in January/February ( $1.3$  °C /century) and the smallest in May/June ( $\sim 0.8$  °C /century). The  
31 duration that the river exceeds the ecologically important threshold of  $20$  °C has increased by  
32  $\sim 20$  days since the 1800s, to  $\sim 60$  d yr<sup>-1</sup>. Moreover, cold water days below  $2$  °C have virtually  
33 disappeared, and the river no longer freezes. Since  $\sim 1900$ , changes are primarily correlated with  
34 increases in air temperature ( $T_w$  increase of  $0.81 \pm 0.25$  °C) but also occur due to increased reser-  
35 voir capacity, altered land use and river morphology, and other anthropogenic changes ( $0.34$   
36  $\pm 0.12$  °C). Managed release of water influences  $T_w$  seasonally, with an average reduction of  
37  $0.27$  °C and  $0.56$  °C estimated for August and September. System changes have decreased daily  
38 variability ( $\sigma$ ) by  $0.44$  °C, increased thermal memory, and reduced interannual variability. These  
39 system changes fundamentally alter the response of  $T_w$  to climate change, posing additional  
40 stressors on fauna.

## 41 Short Summary

42 This manuscript uses archival measurements and a statistical model to show that water tempera-  
43 tures in the Willamette River have trended upwards since 1850, with the largest increase occur-  
44 ring in winter and the smallest in late spring. Approximately 30% of the increase is attributable  
45 to system changes, and 70% to warming air temperature (climate change). The number of warm  
46 water days has significantly increased, and near freezing conditions, common historically, no  
47 longer occur.

## 48 1.0 Introduction

49 Water temperatures are rising in many temperate streams and rivers, in part due to climate  
50 change (e.g., Kaushal et al., 2010). Beyond a warming climate, many additional factors influence  
51 water temperature ( $T_w$ ), including land-use patterns, water withdrawal and return flows, reservoir  
52 storage, and other types of water-resources management (e.g., Olden & Naiman, 2010; Bottom et  
53 al., 2011). Because water temperature influences ecological processes, water quality, oxygen  
54 levels, and fish habitat and survivability (e.g., Caissie, 2006, Bottom et al., 2011), defining long-  
55 term temperature trends and understanding their causes is vital. However, with few exceptions  
56 (e.g., Webb & Noblis, 2007; Pohle et al., 2019), few  $T_w$  records from the late 19<sup>th</sup> or early 20<sup>th</sup>  
57 century have been evaluated, particularly in North America (Kaushal et al., 2010). The limited  
58 availability of earlier records inhibits the ability to discern secular trends, evaluate causes, and  
59 assess impact. There is, therefore, a need to digitize and analyze archival water temperature rec-  
60 ords, such as those collected daily by the US Signal Service in the 1880s at 20+ coastal and river  
61 stations (see the Monthly Weather Review series of publications, volume 9 to 18).



62 In the Pacific Northwest,  $T_w$  controls the long-term viability of salmon and other endangered spe-  
63 cies (Mantua, 2010; Bottom et al., 2011, Isaak et al., 2012, Caldwell et al., 2013). Above a  
64 threshold of 18–21 °C, various species of salmon, steelhead, and trout are stressed and become  
65 more susceptible to disease (OR DEQ, 2006, Mantua, 2010). As a result, regulations require that  
66 the seven day average of the daily maximum temperature should not exceed 20 °C, with a lower  
67 threshold set for rearing and spawning streams (e.g., OR-DEQ, 2006). An allowance of 0.3 °C is  
68 permitted for the sum of all anthropogenic point sources such as wastewater discharge, and non-  
69 point sources such as loss of shading or heating in reservoirs. Hence, the Willamette River in  
70 Portland, Oregon (Figure 1) is considered an impaired water body and out of regulatory compli-  
71 ance for  $T_w$  above 20.3 °C (OR DEQ, 2006).

72 Accurately assessing and disentangling anthropogenic and climate change influences is challeng-  
73 ing because of the large number of alterations and anthropogenic uses (e.g., diversions and dis-  
74 charges), and feedbacks between different factors. Compared to its natural state, the Willamette  
75 River is more channelized, deeper, and reduced in length (particularly in upstream reaches; e.g.,  
76 Sedell and Froggatt, 1984; Benner and Sedell, 1997; Gregory et al., 2002a). The construction of  
77 large storage reservoirs (Payne, 2002) has altered flow patterns and heating patterns within the  
78 basin, and several hydroelectric projects increase  $T_w$  (OR DEQ, 2006). Logging within the water-  
79 shed reduces shading and also increases  $T_w$  (Johnson & Jones, 2000). Nonetheless, summertime  
80 peak  $T_w$  values at reservoir sites likely decreased after dam construction, because of increased  
81 water depths; at the same time, autumn temperatures have increased (e.g., Angiletta et al., 2008;  
82 Rounds, 2010). Below the storage reservoirs, channelization of the Willamette, deforestation of  
83 the riparian corridor (decreased shading) (Gregory et al. 1991, Wallick et al. 2022), water diver-  
84 sions, and storage for agriculture have also likely shifted  $T_w$  (Berger et al., 2004). Because of a  
85 lack of in-situ data from pre-reservoir conditions, the cumulative effect of anthropogenic influ-  
86 ence since European settlement is currently unknown (OR DEQ, 2006).

87 Hydrological and land-use changes in the Willamette Basin have occurred within a background  
88 of a warming climate and hotter extremes. The summers of 2009, 2015, and 2021 were dry and  
89 hot in the Pacific Northwest, with conditions consistent with the future climatology predicted by  
90 climate models (e.g., Mote and Salathé, 2010, Bumbaco et al., 2013). In 2015, snowpack was  
91 extremely low, leading to record low streamflow in many rivers (Mote et al., 2016). The combi-  
92 nation of hot, dry weather and low river discharge produced elevated water temperatures, ad-  
93 versely affecting salmon populations (Crozier et al., 2020). However, despite record heat waves  
94 during the summer of 2021 (Portland reached a record air temperature of 46.7 °C, about 5 °C  
95 above the previous all-time high), water temperatures in the Willamette River, a major tributary  
96 of the Columbia River, did not reach the peak of 2015.

97 Anomalously hot years are useful for understanding processes that control  $T_w$ , and characteriz-  
98 ing natural variability in the context of climate change. How anomalous were water temperatures  
99 in coastal rivers in the Pacific Northwest during 2009, 2015 and 2021, and to what extent has cli-  
100 mate change influenced extremes? How much have water temperatures changed from natural,  
101 background conditions? The dearth of long-term data complicates assessment of patterns and  
102 trends, since weather patterns such as El Nino/La Nina and the Pacific Decadal Oscillation influ-  
103 ence interannual and decadal variability in  $T_w$  (Peterson & Kitchel, 2001). Also, the construction  
104 of reservoirs, deforestation of the riparian corridor, irrigation diversions, and other land-use  
105 changes are known to influence flow hydrographs and  $T_w$  in other basins (e.g., Olden & Naimen,



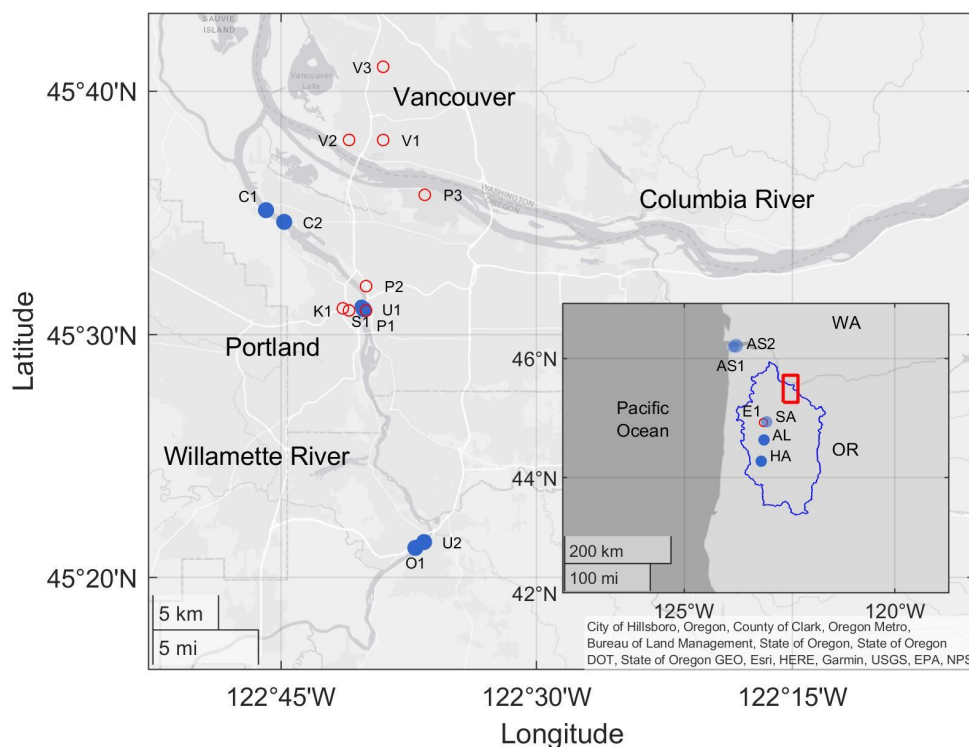
106 2010). Because chronic and acute anthropogenic factors change over time, they may mask or ac-  
107 centuate climate-induced variability and trends in degradation or recovery (NASEM 2022).

108 To investigate the secular changes in water temperatures caused by climate change and local an-  
109 thropogenic influence, we construct a unique, instrument based  $T_w$  data set on the lower  
110 Willamette River (OR) that extends back to 1881, a time period with a cooler climate and unim-  
111 peded, natural flows. Water temperature records were found and digitized from various federal,  
112 state, and local archives, producing ~90 years of daily records stretching over a 140 year period.  
113 Seasonal patterns and long-term trends are assessed, and their relationship to local air tempera-  
114 tures are evaluated using a stochastic regression approach. Results show that extreme summer-  
115 time water temperatures similar to 2009 and 2015 are found in the historical record (e.g., 1889  
116 and 1941), and that water temperatures have frequently exceeded 20 °C during the summer, even  
117 in the 19<sup>th</sup> century. However, on secular time scales, average water temperature is rising during  
118 all times of the year, and the number of warm-water days is increasing. Therefore, temporal re-  
119 fugia during the time periods most conducive to coldwater species are becoming increasingly  
120 scarce.

## 121 2. Background and Methods

### 122 2.1 Setting

123 The Willamette River (Figure 1), with a mean annual discharge of 940 m<sup>3</sup>/s (1971– 2020 period),  
124 drains approximately 29,700 square km of coastal Oregon (Figure 1; Branscomb et al., 2002). It  
125 is the 13<sup>th</sup> largest river in the contiguous United States by volume (Wallick et al. 2022), and its  
126 waters discharge into the larger Columbia River approximately 162km from the Pacific Ocean.  
127 The lower Willamette River, the focus of this study (Figure 1), is an approximately 43 km long  
128 region influenced by ocean tides during low-flow conditions and by backwater from the Colum-  
129 bia River, particularly during spring (Helaire et al., 2019). Because of its location near the  
130 mouth, the lower Willamette is influenced by and integrates climate changes and local anthropo-  
131 genic changes occurring throughout the basin. Their net effect on  $T_w$  is explored in this manu-  
132 script; here, we first review the time history and magnitude of anthropogenic changes.



133

134 *Figure 1: Site map with locations of  $T_w$  (blue, closed circles) and  $T_a$  (red, open circles) measurements.*  
 135 *The red bounding box in the inset denotes the Portland/Vancouver Metropolitan Area depicted in the*  
 136 *larger figure. The Willamette River watershed boundaries are denoted in blue. OR = Oregon, WA =*  
 137 *Washington. Abbreviations and period of record of the measurements are provided in Table 1.*

138 The Willamette Basin has a temperate climate marked by overcast conditions from October–  
 139 May, and predominately sunny, dry conditions from approximately mid-June to mid-September.  
 140 Average annual precipitation on the valley floor is ~100–130 cm/yr., with up to 500 cm occur-  
 141 ing in the Cascade Mountains (Baker et al., 2002). Rainfall occurs primarily between October  
 142 and May, with the wettest period occurring between November and January. At Portland, the  
 143 largest discharge typically occurs during winter storms and peaks in the November–February  
 144 period (Figure 2a). Historically, snow-melt driven flows contributed to elevated flows in the  
 145 March–May time frame (Figure 2a). The combination of declining snowpack (e.g. Mote et al.,  
 146 2018) and water management (e.g., Rounds, 2010) has reduced spring discharge. During sum-  
 147 mer, 60–80% of river water derives from high elevation regions above 1200m, either as direct  
 148 snowmelt or as groundwater (Brooks et al., 2012). Late summer discharge has increased, how-  
 149 ever, because of the managed release of water. In the future, unimpeded wintertime discharges  
 150 are expected to increase while summertime flows decrease (e.g., Chang & Jung, 2010).



151 The lower 300km of the Willamette River runs south-to-north through the Willamette Valley,  
152 which is now primarily agricultural. For thousands of years the Willamette Basin was inhabited  
153 by Native Americans, who influenced the watershed in many ways, including through controlled  
154 burns and small-scale fish dams (Boyd, 1999, Johannessen et al. 1971, Taylor, 1999). European  
155 settlement began in the early 1800s; Portland, founded in 1843, became the largest city in Ore-  
156 gon by 1860 (US Census, 1866). Shading has been reduced in its modern, channelized configura-  
157 tion compared to historical norms (Lee et al. 1995; OR-DEQ 2006). Land under irrigation was  
158 minor before 1910, and increased from ~13,500 hectares in 1945 to about 110,000 hectares by  
159 1979 (Sedell & Froggatt, 1984). East side tributaries such as the Clackamas River (Willamette  
160 Rkm 40), the Mollalla River (Rkm 58) and the McKenzie River (Rkm 282) drain the mountain-  
161 ous Cascade Range, and flow primarily through steep forested regions. West-side tributaries such  
162 as the Tualatin River (Rkm 45) and the Long Tom River (Rkm 240) drain the lower, forested  
163 Coast Range and are slower moving (Lee et al., 1995). The Willamette splits into the Middle  
164 and Coast-fork at ~ Rkm 301; the headwaters of the Middle fork are approximately 486km from  
165 the confluence of the Willamette and the Columbia rivers.

166 The mainstem of the Willamette River has been extensively modified since the latter part of the  
167 19<sup>th</sup> century, first for navigation and agriculture, and later for flood control. Pre-European settle-  
168 ment, the river was maintained in a prairie or savannah-like condition by burning (Christy and  
169 Alverson 2011). After burning ceased (~ late 1700s), the river became fringed by a 3–7 km wide  
170 floodplain covered by a dense riparian forest (Thilenius 1968, Sedell & Froggatt, 1984). In the  
171 1850s, approximately 97,500ha of the Willamette Valley was mapped by the Government Land  
172 Survey Office as riparian and wetland forest, and was dominated by tree species such as *Quercus*  
173 *garryana* (Oregon white oak), *Fraxinus latifolia* (Oregon ash), *Acer macrophyllum* (bigleaf map-  
174 ple), *Alnus rubra* (red alder), and *Populus trichocarpa* (black cottonwood) (Christy and Alverson  
175 2011). The river planform was dynamic; the upper 200km typically contained 2– 5 shallow (1.5–  
176 3 m deep), braided channels that evolved each year due to the formation of gravel bars and drift-  
177 wood barriers (Sedell & Froggatt, 1984; Gregory et al., 2002a; Wallick et al. 2022). Beginning in  
178 the 1870s, but particularly in the first half of the 20<sup>th</sup> century, the river was reduced to a primar-  
179 ily single-thread stream, and shortened by nearly 20km (Sedell & Froggatt, 1984; Gregory et al.,  
180 2002a). Bank-stabilization measures began in the late 1800s and occurred most prominently dur-  
181 ing the mid-20<sup>th</sup> century (1930s– 1960s); approximately 25% of Willamette River banks now  
182 have revetments, armoring, wing dikes, and other bank protection measures (Gregory et al.,  
183 2002b). Further, from 1870– 1950, approximately 65,000 “snags” (30– 60m long trees with a di-  
184 ameter of 0.5– 2m) were removed (>500 per km; Sedell & Froggatt, 1984). Peak snag removal  
185 occurred in the late 1800s/early 1900s (Sedell & Froggatt, 1984). These snags were often used to  
186 block-up side channels. As a result, off-channel areas such as alcoves and sloughs—often 2– 7  
187 °C cooler than the mainstem—have decreased in extent by 70– 80% (Landers et al., 2002). Ad-  
188 ditionally, the forested area in the floodplain has decreased by 75-90% (Landers et al., 2002,  
189 Gregory et al. 2019). Dredging further altered the river, after its authorization in 1906. Between  
190 1908– 1929, approximately 78,000 m<sup>3</sup> yr<sup>-1</sup> of sediment were removed from the river above tide-  
191 water (Willingham, 1983), but much more extensive dredging has occurred in Portland Harbor.  
192 The depth of the river is currently ~ 12m in the lower ~20km of the Willamette, the focus area of  
193 our study (Figure 1). Depths gradually reduce to a centerline depth as shallow as 1.5– 2m  
194 around Rkm 280 (US Geological Survey (USGS), 2003).



195 A total of 371 reservoirs and impoundments of various size have been built in the Willamette ba-  
196 sin, with a combined capacity of more than  $3.3 \text{ km}^3$  (Payne, 2002). Given a mean discharge of  
197 about  $980 \text{ m}^3\text{s}^{-1}$  (Naik and Jay, 2011), these reservoirs store  $\sim 10.6\%$  of the annual average flow.  
198 The majority were built between 1950– 1980, with  $\sim 23$  built pre-1950 and  $\sim 25$  after 1980  
199 (Payne, 2002). Approximately 45% are small storage reservoirs for irrigation (order  $100,000 \text{ m}^3$   
200 capacity); hydroelectric dams ( $\sim 9\%$ ) and water supply reservoirs (6% of total) are typically of  
201 similar size (Payne, 2002). A total of 13 federal reservoirs for storage and flood control were  
202 built between 1941 and 1969 with a combined maximum storage capacity of  $2.75 \text{ km}^3$  (Rounds,  
203 2010); the largest are Detroit Dam (completed 1953, capacity  $0.56 \text{ km}^3$ ), Lookout Point Dam  
204 (completed 1954, capacity  $0.59 \text{ km}^3$ ) and Green Peter Dam ( $0.53 \text{ km}^3$  capacity, completed 1968;  
205 Payne, 2002; Rounds, 2010). The two federal reservoirs built in the 1940s were relatively small  
206 (combined capacity of  $0.18 \text{ km}^3$ ) compared to modern capacity; therefore, we consider the period  
207 before 1953 to be pre-river flow regulation. An examination of hydrological records suggests  
208 that flood control exerted some influence in the 1954– 1964 period, reducing peak flows during  
209 the December 1964 flood considerably, and that the modern hydrological regime began  $\sim 1965$ –  
210 1970 (Gregory et al., 2002c). In total, reservoirs have increased the surface area of water within  
211 the system by about  $200 \text{ km}^2$ , with the majority (80– 85%) occurring in the 13 federally operated  
212 water projects (Payne, 2002). A net increase of  $\sim 50 \text{ km}^2$  in water surface area is estimated for the  
213 Willamette Valley since 1851 (Gregory et al., 2002d), in part from water impoundments. By  
214 comparison, channelization between 1850 and 1995 only removed  $\sim 17 \text{ km}^2$  of water surface on  
215 the mainstem Willamette, from  $76$  to  $59 \text{ km}^2$  (Gregory, 2002a). Combined with the loss of ripar-  
216 ian corridor shading during the growing season (Gregory et al., 2002e; Rounds, 2007), the in-  
217 creased surface area in the basin means that heat input into the fluvial system—for the same me-  
218 teorological conditions—has increased.

219

## 220 2.2 In-situ water temperature measurements

221 A number of measurements were obtained to assess changes to meteorological and fluvial condi-  
222 tions since the mid-19<sup>th</sup> century (Figure 1; Table 1 & Table 2), and approximately 30 years of ar-  
223 chival records were digitized. From 1881– 1890, the US Signal Service (USSS) measured top-  
224 and bottom  $T_w$  at Portland at 11:00 (local time) every day. The successor to the USSS, the US  
225 Weather Bureau (USWB) measured  $T_w$  from 1941– 1961 between 6:30 am and 7:30 am daily  
226 (local standard time). We digitized and quality assured the previously unanalyzed USSS and  
227 USWB records, which were obtained from the National Centers for Environmental Information  
228 (NCEI). A spot-check of US Army Corps of Engineers records from Willamette Rkm 10.5 from  
229 1941– 42 (Moore, 1968) showed a general consistency with USWB measurements, to within  $1^\circ$   
230 C. Measurements of  $T_w$  are available from the US Geological Survey (USGS) since 1961, with  
231  $\sim 26$  station years available in the Portland metropolitan area since 1971 (Table 1). Such federal  
232 records are supplemented by additional state and local records. Intermittent Grab-sample meas-  
233 urements of  $T_w$  are available from the State of Oregon Department of Water Quality, particularly  
234 during summer (1949, 1953– present; obtained from the City of Portland). Nearly continuous  
235 daily measurements of  $T_w$  at the Willamette Falls fish ladder from 1985– 2020 were obtained  
236 from the Oregon Department of Fish and Wildlife. Finally, a long, continuous record has been  
237 made available by the City of Portland at half-hourly increments from 1992– 1999 and 1997–



238 2015 at the Saint Johns Bridge and the St Johns Railroad Bridge, respectively (see also Annear et  
239 al., 2003).

240 Water temperature records from these different locations are combined together to obtain a 90  
241 year record of in-situ  $T_w$  covering 64% of the 1881 to 2021 period (Table 1). Once-a-day meas-  
242 urements were adjusted to the daily minimum temperature, because most historical measure-  
243 ments were made in the morning. The adjustment, typically  $\sim 0.1$  °C, was based on the monthly  
244 averaged differences between measurement time stamps and the daily minimum in modern, high  
245 resolution data (Table 1). The composite 1881– 2021 record uses lower Willamette records when  
246 available, and the nearest data otherwise (if available). Records in Oregon City and further up-  
247 stream were adjusted for spatial heating effects through the use of monthly averaged gradients  
248 observed between coterminous measurements from 2000– 2017. Most adjustments for spatial  
249 variability were minor ( $< 0.3$  °C), except for a few years (1962, 1983– 1984) in which the only  
250 available measurements were from the middle or upper Willamette River. Additional notes are  
251 included in Table 1, and the source of data in the composite are included in the data record (see  
252 supplement).

253 Additionally, we use  $T_w$  measurements from the lower Columbia River to check our model esti-  
254 mates (see section 2.4) during periods with no other data (Figure 1, Table 1). Water temperature  
255 was measured up to twice daily at Astoria from 1854– 1876 (Talke et al., 2020), approximately  
256 24 km from the present-day mouth. Monthly estimates of  $T_w$  at Astoria, Tongue Point (Rkm 29)  
257 are available from 1925– 1964 (USC&GS, 1967), and daily records were obtained from 1940–  
258 42 (Moore, 1968) and 1949– present from the National Oceanographic and Atmospheric Admin-  
259 istration. Before 1950, surface waters at Astoria were generally freshwater or brackish during  
260 typical flow conditions (Al-Bahadily, 2020, USC&GS, 1967), and therefore approximate river  
261 water temperatures. During the November– April rainy season, good agreement is found be-  
262 tween model results and Astoria measurements, thus helping to validate the model. During other  
263 times of year, snow melt from the interior Columbia River basin dominates the river flow signal  
264 (e.g., Naik & Jay, 2011; Helaire et al., 2019), suppressing water temperature (see Results, Sec-  
265 tion 3). Additional information about the Astoria measurements is given in Talke et al. (2020)  
266 and Scott et al. (2022).

267 Monthly averages of the USGS, DEQ, and City of Portland data from 2009 to 2015 agree to  
268 within 0.1– 0.2 °C, indicating that modern measurements from the last two decades are con-  
269 sistent and of high quality. This comparison also shows that grab samples from the water surface  
270 compare favorably with other methods. Measurements by the USSS (1881– 1890) and USWB  
271 (1941– 1961) were made at a 1<sup>st</sup>-order weather station by trained professionals, and appear to be  
272 of high quality; however, little independent verification is possible. Evaluation of data from  
273 1962 to the mid-1990s indicates some periods with lesser quality in which different measure-  
274 ments disagree with each other. For example, summertime measurements from a thermograph in  
275 Oregon City (1963– 1967) are as much as 1.8 °C higher (monthly average) with coterminous  
276 grab-samples; a smaller, but still significant, bias is found between Saint Johns Bridge measure-  
277 ments (1971– 1975) and grab-samples (Table 1). Since the typical difference between such  
278 measurements is reported to be  $< 1$  °F (0.56 °C) (Moore, 1967), some unknown issue occurred.  
279 The availability and quality of in-situ data informs our choice of model calibration periods and  
280 interpretation of model/data comparisons.





281 *Table 1: In-situ water temperature measurements used to obtain a composite record of daily minimum water tem-*  
 282 *perature in Portland, 1881– 2020. Locations ordered based on start-date and originating agency.*

Location	Originating agency	Short name	River km	Latitude	Longitude	Measurement Dates	Measurement Frequency	Precision	Bias Correction
Astoria Downtown <sup>a</sup>	US Coast Survey	A1	CR. 24	46.19	-123.829	6/1854– 10/1876	Various, usually 6:00 am and 6:00 pm daily	±0.03 °C	None applied
Stark Street, Portland <sup>b</sup>	US Signal Service	S1	21	45.519	-122.671	9/1881 – 11/1890	11:00 am daily	±0.3 °C	0.1 °C to 0.2 °C
Astoria Tongue Point	US CGS (pre-1973) & NOAA	A2	CR 29	46.207	-123.768	1/1925– present; daily to 1995, hourly 1995– present	Monthly 1/1925– 12/1964; Daily 11/1940– 6/1942, 01/1949– 12/1995; Hourly 11/1993– present	±0.2 °C before 1994; ±0.03 °C modern	None applied
Morrison Street Bridge, Portland <sup>b</sup>	US Weather Bureau	W1	21	45.517	-122.668	7/1941 – 10/1961	7:30 am daily (except Sunday)	±0.3 °C	0 °C to 0.2 °C
Lower Willamette River <sup>d</sup>	Oregon Department of Environmental Quality	D1	19– 21 (primarily)	Various	Various	1949– 2015; 2746 grab samples retained after quality assurance	6:00am– 12:00 pm; mode = 9:00 am. monthly in winter, once weekly in summertime	±0.1 °C	Median 0.1 °C; 90% corrections < 0.2 °C
Harrisburg	USGS Gauge 14166000		259	44.2704	-123.174	6/1961– 9/1987 10/2000– Present	Daily Max, Min & Mean	±0.05 °C	
Oregon City	USGS Gauge 14207770	U2	42	45.3578	-122.610	3/1963– 9/1967	Daily Max, Min & Mean	±0.05 °C	0.7– 1.8°C Diff. w/Grab samples during summer
Salem	USGS Gauge 14191000	SA	137	44.9442	123.0429	10/1963 – 9/1987	Daily Max, Min & Mean	±0.05 °C	
Saint Johns Bridge	USGS Gauge 14211805	U3	9	45.583	-122.759	10/1971– 9/1975	Daily Max, Min & Mean	±0.05 °C	0.6– 1.05 °C Diff. w/Grab samples during summer
Morrison Street Bridge, Portland	USGS Gauge 14211720	U1	21	45.5175	-122.669	11/1975– 9/1981 11/2001– 9/2005 01/2009– Present	Daily Max, Min & Mean through 2005. Every 30 minutes	±0.05 °C	None applied
Willamette Falls Fish Ladder <sup>e</sup>	Oregon Department of Fish and Game	O1	43	45.354	-122.618	01/1985– present	Not tabulated; Daily, with gaps	± 0.2 °C	-0.3 to 0.3 °C, based on monthly difference with Portland
Saint Johns Bridge <sup>f</sup>	City of Portland, BES	C1	9	45.585	-122.765	7/1992 – 9/1999	Every 30 minutes	± 0.01 °C	Very biased; not used.
Saint Johns Railroad Bridge <sup>f</sup>	City of Portland, BES	C2	11	45.5773	-122.747	9/1997– 9/2012	Every 15 minutes	± 0.01 °C	Averaged with USGS record
Albany	USGS Gauge 14174000	AL	192	44.6388	-123.107	08/2001– Present	Daily Max, Min & Mean	±0.05 °C	

283 Notes: Stations ordered by start date, with earliest measurements first. All times given in local standard time. Bias corrections are subtracted  
 284 from raw measurements on a monthly basis to obtain daily minimum; a positive value indicates a downward adjustment. Coordinates provided in  
 285 the North American Datum of 1983. The locations for the measurements at Stark Street, Astoria Downtown, Willamette Fish ladder and the City  
 286 of Portland measurements are estimated based on available data. River km are the thalweg distance from the mouth of the Willamette, except for  
 287 Astoria which is on the Columbia River.

288 *Specific Footnotes:* (a) Measurements obtained from US National Archives; see Talke et al., 2020; (b) Measurements obtained from National  
 289 Centers for Environmental Information; (c) Data obtained from NOAA; Grab samples from 1925– 1995, approximately daily, generally between  
 290 10:00am – 1:00pm; median ~11:30 am.(d) Data obtained from US EPA Storet database. Measurements often made from bridges in the Portland  
 291 Metro area, including the Hawthorne Bridge, the Steel Bridge, and SPSS Railway Bridge. Samples pre-1960 discarded because of lack of time  
 292 stamp. Grab samples after 12:00 pm (noon) not considered to avoid afternoon heating signal. Pre-12:00 pm data adjusted to daily minimum on  
 293 monthly basis based on modern USGS data. Measurements at 1– 3 day frequency in 1964– 1972; (e) Data from 1985– 1999 obtained directly  
 294 from agency; post 1999 records available online. Based on a comparison using 2001–2004 data, an average warming of 0.2 to 0.3 °C occurs be-  
 295 tween Willamette Falls and Portland from July to September. A cooling of up to 0.3 °C occurs between March to May. Little variation occurs at  
 296 other times; (f) Obtained directly from agency; pre-2000 data also obtained from Berger et al., 2004.



## 297 2.2.2 Meteorological and Flow records

298 A nearly complete record of discharge in the lower Willamette River is available from 1893–  
299 present, with less certain estimates from 1853– 1892. Daily discharge is available from the  
300 USGS in Portland from 1972 to the present (USGS Gauge 14211720). Routed estimates of dis-  
301 charge are available for earlier periods from 1878 forward from Jay & Naik (2011), based on  
302 USGS measurements at Albany (USGS Gauge 14174000) and Salem (USGS gauge 14191000).  
303 Routed estimates pre-1893 are less certain, because of gaps in the record (Jay & Naik, 2011).  
304 Daily Portland water level measurements are available from 1876– present, and estimates of 30d  
305 averaged Portland water level are available from 1855– 1876 based on tidal measurements at As-  
306 toria (Talke et al. 2020). Nineteenth century measurements incorporate a substantial backwater  
307 effect from the Columbia River that historically varied from zero to as much as 10 m during  
308 some spring freshet events (see Helaire et al., 2019).

309 Records of daily maximum  $T_a$  from the Portland-Vancouver area were found in several sources  
310 (Table 2). Continuous daily weather records at Vancouver (1849– 1868) and Eola (1870– 1892)  
311 were measured by the USSS and were provided in digital form by the Midwestern Regional Cli-  
312 mate Center (<https://mrcc.purdue.edu/>). Additional daily records from the USWB and the Na-  
313 tional Weather Service from Portland and Vancouver cover the 1874– present period and were  
314 obtained from NCEI.

315 Air temperature records were carefully evaluated for potential bias (e.g., caused by elevation dif-  
316 ferences) and consistency with each other (Table 2; see Figure 1 for locations). For example, the  
317 Vancouver record from 1895– 1965 is on average ~0.4 to 0.5 °C warmer than the downtown  
318 Portland record. The Portland Airport reading was <0.05 °C cooler than the downtown Portland  
319 Weather Bureau reading between 1940– 1948, on average. Thereafter, the Portland Weather Bu-  
320 reau record warmed more quickly, and was 0.54 °C warmer than the Airport from 1960– 1969.  
321 The modern Portland KGW record (1973– present), located at 48.5m above sea-level, is slightly  
322 cooler from 1991– 2020 (annually averaged daily maximum = 17.08 °C) than the Portland Air-  
323 port (17.47 °C). Under standard atmospheric conditions, with a lapse rate 6.5 °C per 1000m, a  
324 difference of ~0.3 °C is expected between these records. Thus, we conclude that the measured  
325 difference between the stations is almost entirely explainable by elevation effects. After adjust-  
326 ing for mean biases, the root-mean-square error observed between the different Portland air tem-  
327 perature records is around 1– 1.1 °C from 1940– present. Daily maxima between Vancouver and  
328 Portland show more variability (RMSE of ~1.5– 1.6 °C), possibly because of small differences in  
329 climate. The influence of these small differences on our  $T_w$  model results are explored later.

330

331



332 *Table 2: Meteorological stations used to develop statistical models, and associated root mean square*  
 333 *error (RMSE) of water temperature obtained for different calibration periods (annual, summer, and win-*  
 334 *ter). The RMSE represents either the daily or monthly averaged difference with in-situ water temperature*  
 335 *measurements, in degrees Celsius. Station Identification numbers (ID) are from the US National Weather*  
 336 *Service. Measurement dates denote the time period that daily maximum temperature was recorded at*  
 337 *the given location. The latitude/longitude value for Eola (near Salem, Oregon) is estimated. All stations*  
 338 *except Vancouver are in Oregon.*

Name	Station ID	Measurement Dates	latitude	longitude	Model Name	Calibration Period	RMSE Annual Calibration (°C)	RMSE Summer Calibration (°C)	RMSE Winter Calibration (°C)	RMSE Annual (monthly avg) (°C)	RMSE Summer (monthly avg) (°C)	RMSE Winter (monthly avg) (°C)
<b>Portland Downtown</b>	USW00024274	1874– 1902	45.5166	-122.6667	1881D	1881–1890	1.1	1.2	0.87	0.78	0.92	0.5
<b>Portland Downtown</b>	USW00024274	1902– 1973	45.5333	-122.6667	1941D	1941–1952	0.91	0.68	0.75	0.62	0.48	0.43
<b>Portland Airport</b>	USW00024229	1938– 2021	45.5958	-122.6093	1941A	1941–1952	0.91	0.66	0.78	0.6	0.46	0.42
<b>Portland Airport</b>	USW00024229	1938– 2021	45.5958	-122.6093	2000A	2000–2015	0.88	0.51	0.75	0.62	0.31	0.48
<b>Portland KGW<sup>2</sup></b>	USC00356749	1973– 2021	45.5181	-122.6894	2000D	2000–2015	0.87	0.53	0.72	0.62	0.33	0.46
<b>Vancouver, Washington<sup>3</sup></b>	USC00458773	1849– 1868 1891– 1966	45.6333	-122.6833	1941V	1941–1952	0.98	0.75	0.85	0.68	0.54	0.48
<b>Eola</b>	US Signal Service Observation	1870– 1892	44.9323	-123.1198	1881E	1881–1890	1.22	1.41	1.05	0.91	1.17	0.72

339 Notes:

340 1. The annual RMSE between measurements and the climatological average is 1.86, 1.46, and 1.43 °C for the 1881– 1890, 1941– 1952, and  
 341 2000– 2015 calibration periods, respectively.

342 2. The 1973– 1999 measurement was at a slightly different location of (45.517W, -122.683E). The elevation of the 1973– present dataset is  
 343 ~48.5m. The lapse rate for the standard atmosphere (6.5 °C per 1000m) suggests that the difference to a measurement at sea-level is ~0.3 °C. An  
 344 observed difference in average daily maximum temperature at the Portland Airport (17.46 °C, <10m relative to sea-level) and Portland KGW  
 345 (17.07 °C) between 2000– 2020 is therefore mostly caused by elevation differences.

346 3. The Dec. 1849– 1868 measurement at Fort Vancouver was made by the US Signal Service; the approximate location was 45.633N, -122.65E,  
 347 and was several km east of the 1891– 1966 measurement. The gauge was moved in 1966 to a higher elevation location with a known bias (Mote  
 348 et al., 2002). The 1966– present data is therefore not used.

349

### 350 2.3 Advection-Diffusion equation

351 To develop our statistical model approach, understand its limitations, and motivate its form, we  
 352 first consider the underlying physical dynamics. Heating and cooling of river water is governed  
 353 by the Advection-Diffusion equation (ADE; e.g., Fischer et al., 1979). When vertical and cross-  
 354 sectional variations in  $T_w$  are neglected, the 1-D ADE for  $T_w$  as a function of time  $t$  and along-  
 355 channel coordinate  $x$  (positive downstream) reads:

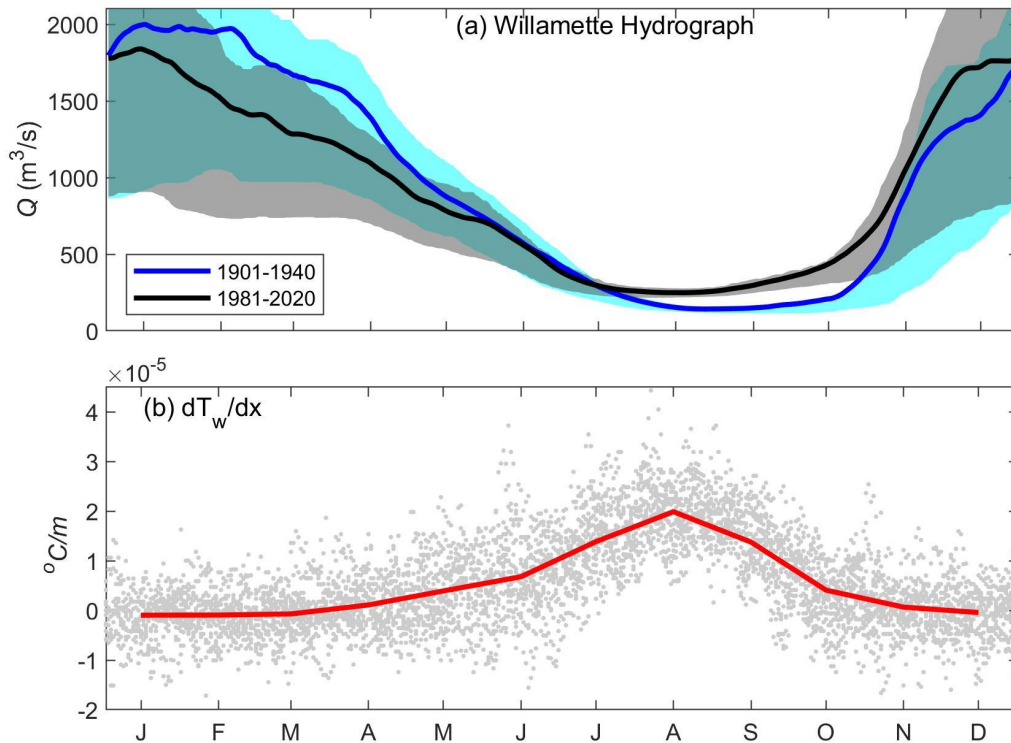


$$356 \quad \frac{\partial T_w}{\partial t} = \underbrace{-u \frac{\partial T_w}{\partial x}}_{\text{Advective Term}} + \underbrace{\frac{\partial}{\partial x} \left( K \frac{\partial T_w}{\partial x} \right)}_{\text{Diffusive Term}} + \underbrace{\frac{H}{\rho c_p d}}_{\text{Heating term}}, \quad (1)$$

357 where  $K$  is a horizontal diffusion coefficient,  $u$  is river velocity,  $H$  is the sum of heat flux into or  
 358 out of the system,  $d$  is the cross-sectionally averaged depth, and  $c_p$  is the heat capacity of water,  
 359 and is approximately constant to within 1% for typical variations in  $T_w$ . This simple ADE does  
 360 not consider groundwater flow, which cools the off-channel alcoves of the Willamette River dur-  
 361 ing summer (Faulkner et al., 2020).

362 Scaling provides insight into the relative importance of the advection, diffusion, and heating  
 363 terms, relative to the time rate of change  $\frac{\partial T_w}{\partial t}$ . Over a 12 hour time scale during the day, tempera-  
 364 tures in summer are observed to vary by  $\sim 0.5$  °C, yielding  $\left(\frac{\partial T_w}{\partial t}\right)_{\text{daily}} \sim 10^{-5}$  °C/s. Over a month,  
 365 larger changes of order 5 °C are observed, yielding  $\left(\frac{\partial T_w}{\partial t}\right)_{\text{monthly}} \sim 2 \times 10^{-6}$  °C/s. The time rate of  
 366 change for daily and monthly time scales must be balanced by the terms on the right hand side of  
 367 Equation (1). An evaluation of measurements suggests that:

- 368 • The diffusive term is negligible. Over most of the year, the monthly average of daily  $\frac{\partial T_w}{\partial x}$   
 369 is  $\ll 10^{-5}$  °C/m, except from July– September when a monthly-averaged increase of 1– 2  
 370 °C per 100km is observed (Figure 2b). Using 100km as a typical length scale and  $K \sim 1000$   
 371  $\text{m}^2/\text{s}$  for the diffusive term, the  $\frac{\partial}{\partial x} \left( K \frac{\partial T_w}{\partial x} \right)$  term is generally  $< 10^{-7}$  °C/s, much less than  
 372  $\frac{\partial T_w}{\partial t}$ .
- 373 • The nonlinear advective term is likely influential during summer, due to a positive  $\frac{\partial T_w}{\partial x}$   
 374 (Figure 2b). During other seasons, river discharge can either cool or warm Portland water  
 375 because of the presence of both negative and positive  $\frac{\partial T_w}{\partial x}$  (Figure 2). Therefore, the net  
 376 influence of the advective term on monthly averaged temperatures is likely small, though  
 377 it may matter during weather events (such as a rain-on-snow event).
- 378 • Seasonal variations in discharge (Figure 2a) influence the magnitude of the advective  
 379 term. During early summertime (June) conditions, Lee (1995) measured velocities of  
 380  $\sim 0.8$  m/s in the upper Willamette; tidally averaged currents are typically 0.05– 0.1 m/s  
 381 during the same period in Portland (USGS Gauge 14211720). Since discharge is smallest  
 382 during August/September, the decrease in  $u$  counteracts the increase in  $\frac{\partial T_w}{\partial x}$  in the advective  
 383 term  $u \frac{\partial T_w}{\partial x}$ . Overall, considering typical magnitudes of  $u$  and  $\frac{\partial T_w}{\partial x}$ , we find that the  
 384 advective term scales as  $10^{-5}$  °C/s to  $10^{-6}$  °C/s during the summer, depending on location.  
 385
- 386 • Based on the considerations above, the heating term is usually the leading order term that  
 387 drives the time rate of  $T_w$ , as also found, for example, by Wagner et al., (2011).  
 388



389

390 *Figure 2: (a) The Willamette hydrograph at Portland, Oregon for the pre-reservoir (1901– 1940) and*  
 391 *modern (1981– 2020) periods, and (b) the horizontal  $T_w$  gradient between Albany, Oregon and Portland*  
 392 *Oregon for the 2000– 2017 time period. Positive indicates that downstream measurements in Portland*  
 393 *are warmer. Shading in (a) denotes the 25<sup>th</sup> and 75<sup>th</sup> percentile of measured discharge. The along-river*  
 394 *distance between Portland and Albany is 169 km. The red line in (b) denotes the monthly average. Tick*  
 395 *marks denote the middle of each month.*

396 When advection and diffusion are unimportant, the non-linear heating term ( $\frac{H}{\rho c_p d}$ ) governs the  
 397 time rate of change of temperature,  $\frac{\partial T_w}{\partial t}$ . The  $\frac{H}{\rho c_p d}$  term can be linearized using a number of as-  
 398 sumptions, enabling use of a linear regression approach in which  $T_w$  is a function of  $T_a$  and river  
 399 discharge  $Q$ . The details, described briefly below, reveal some inherent limitations. See  
 400 Mohseni & Stefan (1999) for a more detailed discussion of linearization assumptions.

401

402 First, we make the approximation that the reciprocal of depth,  $1/d$ , is a function of  $Q$ :

403 
$$\frac{1}{d} \approx a_1 - a_2 Q, \quad (2)$$



404 where  $a_1$  and  $a_2$  are constants. The negative sign reflects the observation that  $1/d$  decreases  
405 (depth increases) as discharge  $Q$  increases.

406 Further, the heat flux term is a function of at least 5 different terms (e.g., Fischer et al., 1979):

$$407 \quad \sum H = H_s + H_e + H_{LW,gain} + H_{LW,loss} + H_{sw} . \quad (3)$$

408 The sensible heat flux is proportional to the difference between air temperature  $T_a$  and  $T_w$  (both  
409 measured in Celsius):

$$410 \quad H_s = k_1 w (T_a - T_w), \quad (4)$$

411 where  $k_1$  is a constant that depends on air density and several empirical coefficients, and  $w$  is the  
412 wind speed at 10m. The energy loss because of evaporative heat flux,  $H_e$ , depends on wind  
413 speed, the latent heat of evaporation, and atmospheric conditions, and is generally small in win-  
414 ter but potentially significant in summer (Wagner et al., 2011). The third term, the heat input  
415 from radiation from water vapor, is

$$416 \quad H_{LW,gain} = k_{LW,gain} (273.15 + T_a)^6 \propto k_{LW,gain} T_a, \quad (5)$$

417 Where  $k_{LW,gain}$  is a constant that depends on cloud cover. When  $\Delta T_a$  is small relative to  
418  $(273.15 + T_a)$ , such as occurs in the Willamette, Equation 5 is approximately linear with respect  
419 to  $T_a$ . Similarly, heat loss due to long-wave radiation is modeled as

$$420 \quad H_{LW,loss} = k_{LW,loss} (273.15 + T_a)^4 \propto k_{LW,loss} T_a, \quad (6)$$

421 where the power term is approximately linear in  $T_a$  for temperature differences  $< 20$  degrees Cel-  
422 sium (see also Mohseni & Stefan, 1999). Finally, the heat input from incoming shortwave radi-  
423 ation,  $H_{sw}$ , is a function of sun angle, albedo, and atmospheric effects. Wagner et al. (2011) used  
424 the climatologically averaged insolation as a basis function in their  $T_w$  model, but most models  
425 implicitly assume that  $H_{sw} R$  is proportional to  $T_a$ , (Benyahya et al., 2007).

426 Combining Equations 3 to 6, and neglecting the evaporation term, we find that  $H$  can be linear-  
427 ized as follows:

$$428 \quad H(t) \approx b_1 T_a + b_2 T_w + b_3 + error, \quad (7)$$

429 where  $b_1$ ,  $b_2$ , and  $b_3$  are constants.

430 Combining Equation 7 and Equation 2, the heating term can be approximated by:

$$431 \quad \frac{H}{\rho c_p d} \approx c_1 T_a + c_2 T_w - c_3 Q T_w + c_4 Q T_a + \epsilon, \quad (8)$$

432 Where  $\epsilon$  is the approximation error and  $c_1$ ,  $c_2$ ,  $c_3$ , and  $c_4$  are coefficients. Equation 8 shows that  
433 even after many simplifications and approximations, there are still nonlinear interactions be-  
434 tween terms such as air temperature and river flow (i.e., the  $Q T_a$  term). In practice, it is found



435 or assumed that air temperature is the most important factor in heating, and only the  $T_a$  depend-  
436 ence is retained (e.g., Erickson & Stefan, 2000, Webb et al., 2003). Most statistical models im-  
437 plicitly start with this assumption, though some non-linear regression approaches have been ap-  
438 plied (see review by Benyahya et al., 2007). For our purposes here, we note that simplifying  
439 heating to be a linear function of  $T_a$  works best during periods of relatively constant water tem-  
440 peratures and river discharge (see also Mohseni & Stefan, 1999). This is one reason why models  
441 calibrated to a specific season such as summer often works better than a model fit to an entire  
442 year (see below).

443 The advection term in Equation 1 can similarly be linearized by assuming that either  $\frac{\partial T_w}{\partial x}$  or  $Q$  is  
444 constant or slowly varying, relative to the other. This yields either a regression term in  $Q$  or in  
445  $T_w$ . Removing nonlinear terms, the following linearized basis function emerges:

$$446 \quad \frac{\partial T_w}{\partial t} = b_w T_w + b_a T_a - c_Q Q, \quad (9)$$

447 where  $b_w$ ,  $b_a$ , and  $c_Q$  are coefficients and the minus sign indicates that river flow reduces water  
448 temperature. Using the approximation  $\frac{\partial T_w}{\partial t} \approx \frac{T_{wn} - T_{wn-1}}{\Delta t}$ , we find that  $T_w$  at time step  $n$  is equal to  
449 the  $T_w$  at the previous time step  $n-1$ , plus a correction that is a function of  $T_a$  and  $Q$ :

$$450 \quad T_{wn} = T_{wn-1} + \Delta t b_w T_{wn} + \Delta t b_a T_a - \Delta t c_Q Q \quad (10)$$

451 This is an autoregressive (AR1) process. Hence, at time  $n-1$ ,  $T_w$  is a function of the  $T_w$  at time  
452  $n-2$ , and the  $T_w$  at  $n-2$  depends on  $T_w$  at  $n-3$ . If we develop and then substitute the solutions  
453 for  $T_{wn-1}$ ,  $T_{wn-2}$ , ... into Equation 10, we find that

$$454 \quad T_w(t) = \sum_{\tau=0}^{\tau=j} a_\tau (t-\tau) T_a(t-\tau) + \sum_{\tau=0}^{\tau=j} b_\tau (t-\tau) Q(t-\tau) + C, \quad (11)$$

455 where  $a_\tau$  and  $b_\tau$  are regression coefficients at some time lag  $\tau$ ,  $C$  is a constant of regression,  
456 and the time period  $j$  is chosen to be long enough that the coefficients  $a_\tau$  and  $b_\tau$  effectively be-  
457 come negligible and/or statistically insignificant. The coefficients  $a_\tau$  and  $b_\tau$  can be modeled us-  
458 ing an exponential filter approach (e.g., Al-Murib et al., 2019); here, as explained below, we esti-  
459 mate the coefficients directly. At a large time lag, the influence of the time-lagged temperature  
460 term in Equation 10 becomes negligible and drops out; hence Equation 11 effectively represents  
461  $T_w$  as a function of time lagged  $T_a$  and river discharge.

462 The discussion above suggests that linear regression models have a basis in the underlying physi-  
463 cal dynamics (see also Mohseni & Stefan, 1999). However, a number of assumptions and ap-  
464 proximations must be made to represent the 1D ADE as a linear model. Factors such as wind,  
465 evaporation, time or spatial variation in parameters and heating terms, and alterations in depth  
466 are only approximately represented by  $T_w$  and  $Q$ . Moreover, depending on conditions, different  
467 terms (e.g., depth, heat flux, and velocity) may contribute in varying degrees to the overall heat  
468 balance. Thus, a linearized representation of average conditions during a particular season may  
469 work less well under unusual or extreme conditions.

470



## 471 2.4 Statistical Model

472 Statistical models are often used to interpret and predict  $T_w$  patterns, using a number of different  
 473 regressions, statistical approaches, or machine learning (e.g., Benyahya et al., 2007, Zhu et al.,  
 474 2018). Within the Pacific Northwest, many studies have developed statistical regression models  
 475 which use  $T_a$  and sometimes also river discharge  $Q$  to model measured  $T_w$  (Moore 1967; Donato,  
 476 2002; Bottom et al., 2011; Mayer, 2012). Such models are simple and run quickly, enabling  
 477 evaluation of time-periods for which in-situ measurements are unavailable and allowing interpre-  
 478 tation of primary forcing factors.

479 We employ a stochastic modeling approach (e.g., Caissie et al., 1998; Benyaha et al., 2007) in  
 480 which the dependent variable (water temperature  $T_w$ ) and the independent variables (air tempera-  
 481 ture  $T_A$  and river discharge  $Q$ ) are decomposed into a long term climatological average and a  
 482 time varying component. A similar approach has also been applied to the Columbia River (Scott,  
 483 2020; Scott et al., 2022). For a generic variable  $X(t)$  measured daily, the climatological average is  
 484 defined as,

$$485 \overline{X(t)} = \frac{1}{y_2 - y_1 + 1} \int_{y_1}^{y_2} \int_{-T/2}^{T/2} X(t) dt dy, \quad (12)$$

486 where  $T = 30$  days,  $t$  is the integer number of days since the start of the year,  $y_1$  is the beginning  
 487 year of the time series (e.g., 1881),  $y_2$  is the end year (e.g., 1890), and the overbar represents the  
 488 climatological average. The number of years in the average should be long enough to capture  
 489 natural variability, but short enough to be statistically stationary (i.e., not overly influenced by  
 490 land use changes or climate change). The 95% uncertainty in the climatological average is given  
 491 by  $\frac{t_* \sigma}{\sqrt{N}}$ , where  $t_* = 1.96$  for a large sample size  $N$ , and  $\sigma$  is the standard deviation. In practice,  
 492 the number of years we used to define the climatological average is limited by available data.

493 The deviation from climatology, caused for example by a heat wave, is defined as:

$$494 X'(t) = X(t) - \overline{X(t)} \quad (13)$$

495 The climatological average for water temperature,  $\overline{T_w(t)}$ , is a good first approximation for condi-  
 496 tions at any given year-day, and correctly estimates daily  $T_w$  in Portland to within a root-mean-  
 497 square-error (RMSE) of  $\sim 1.5$  to  $2$  °C. For a model to have predictive and explanatory power, it  
 498 must exhibit an RMSE significantly less than this climatological average. Present-day numerical  
 499 models typically fulfill this criterion and have an RMSE  $< 1$  °C (Dugdale et al., 2017). To obtain  
 500 comparable error statistics, we rewrite Equation 11 in terms of deviations of  $T_w$  from climatol-  
 501 ogy, and form the following basis function:

$$502 T_w'(t) = \sum_{\tau=0}^{\tau=j} a_{\tau}(t - \tau) T_a'(t - \tau) + \sum_{\tau=0}^{\tau=j} b_{\tau}(t - \tau) Q'(t - \tau) + C, \quad (14)$$

503 where the prime indicates a deviation from climatology and other terms are as defined in Equa-  
 504 tion 11. Based on experimentation, we use daily  $T_a'$  out to two weeks. Thereafter, we use aver-  
 505 age  $T_a'$ , to obtain a statistically significant correlation. A 15 day average is used for day 15– 30,  
 506 and 30 day averages are used thereafter, up to 6 months. Similarly, river discharge  $Q'$  is averaged





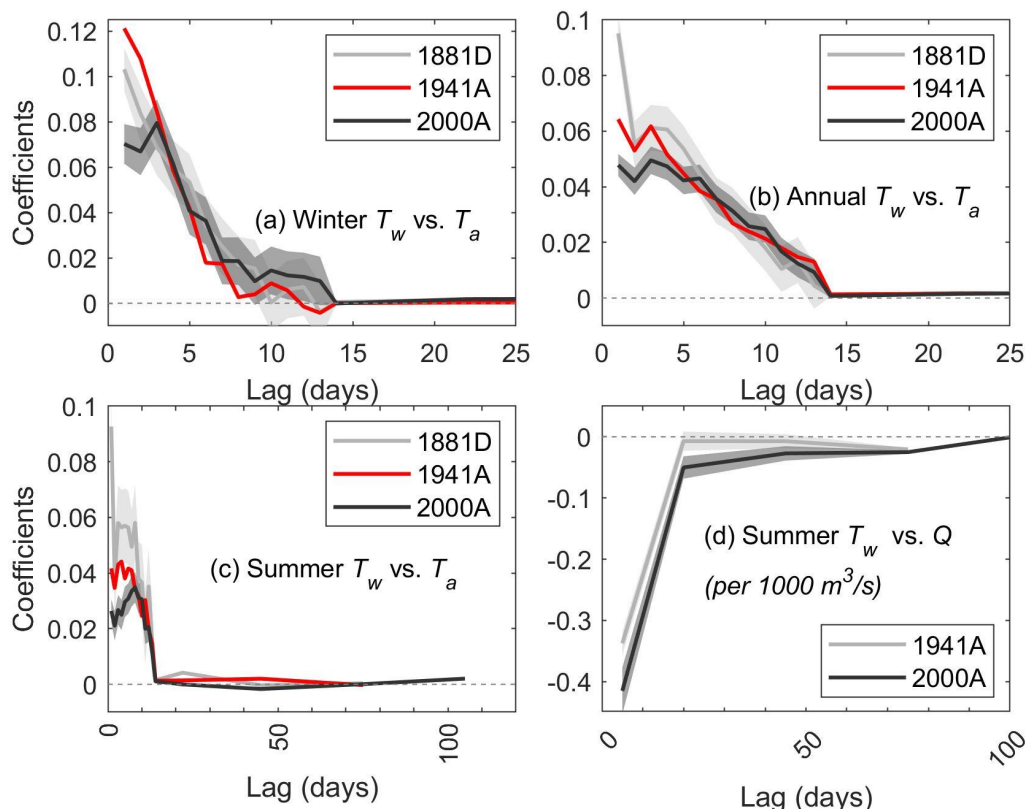
507 using a 10 day average for day 1– 10, a 20 day average for day 11– 30, and – a 30 day average  
508 thereafter.

509 A total of 8 statistical models are developed, based on data from the 19<sup>th</sup> century (1881– 1890),  
510 mid-20<sup>th</sup> century (1941– 1952), and modern period (2000– 2015) (see Table 2). These periods  
511 were chosen based on available data; they approximate (nearly) pre-development conditions, pre-  
512 flood control conditions, and modern conditions. With-in each model, we further divide the year  
513 into a summer sub-model (July– September), a winter sub-model (January– March) and an an-  
514 nual model, based on all available data. Experimentation was used to obtain the optimal winter  
515 and summer models. For example, including June or October into the summer model signifi-  
516 cantly reduced goodness of fit and the statistical influence of river discharge, consistent with the  
517 observation that the horizontal temperature gradient is largest from July to September (Figure  
518 2b). Through experimentation, we also determined that discharge only produces a statistically  
519 significant effect for summertime models based on 1941– 1952 and 2000– 2015 data. This result  
520 is consistent with previous studies (e.g., Isaak et al., 2012) and with estimates of  $\frac{\partial T_w}{\partial x}$  (section  
521 2.3, Figure 2) which suggests that discharge effects are most prominent in summer.

522 Results show that the best-fit coefficients generally decrease in magnitude as  $T_a$  (Figure 3a,b,c)  
523 and river discharge (Figure 3d) are lagged backwards in time. Further, the decorrelation structure  
524 is different for the 19<sup>th</sup>, mid-20<sup>th</sup>, and 21<sup>st</sup> century models (Figure 3); hence, for the same forcing,  
525 these statistical models will produce a different output. Statistically significant coefficients are  
526 found at up to 3 month lag in the 1880s model, and 4 months in the others.



527



528

529 *Figure 3: Coefficients for statistical model vs time lag for (a) air temperature ( $T_a$ ) in the winter model*  
 530 *(Nov– Mar); (b)  $T_a$  in the annual model (all months); (c)  $T_a$  in the summer model (July– Sept) and (d)*  
 531 *discharge  $Q$  in the summer model (July– Sept). The 1881 model is calibrated to 1881– 1890  $T_w$  data, the*  
 532 *1941 model is calibrated to 1941– 1952  $T_w$  data, and the 2000 model is calibrated to 2000– 2015  $T_w$*   
 533 *data. The letter denotes whether  $T_a$  data was sourced from Downtown Portland (D) or from the Airport*  
 534 *(A). Similar results are found for the model based on Vancouver air temperature data (not shown). No*  
 535 *statistically significant effect of river discharge was found for winter or annual models, and the 1880s*  
 536 *summer model, and are not shown.*

537 Each statistical model produces an estimate of  $T_w$  over the period of record of its underlying  $T_a$   
 538 record (Table 2; data available as supplemental information). Based on these time series, a com-  
 539 posite estimate of modeled  $T_w$  was produced, as follows. First, for each station, estimates from  
 540 the two seasonal sub-models were combined, with annual sub-model results used at other times.  
 541 To avoid (typically small) discontinuities between sub-models, a 15-day linear relaxation period  
 542 between sub-model start and stop times was applied. Next, a composite estimate for  $T_w$  was  
 543 made for the 1850– 2020 period, using the best available meteorological measurements and sta-  
 544 tistical models. Vancouver measurements were used pre-1868, downtown Portland from 1874 to  
 545 1939, and the Portland Airport data thereafter. Water temperature estimated from Eola  $T_a$  mea-  
 546 surements were used to fill the 1870– 1874 period. A compromise was required when deciding  
 547 which era of model to use in the composite, since there is no clear delineation between pre and



548 post-reservoir conditions, or between a nearly natural and substantially altered landscape. The  
549 mid-20<sup>th</sup> century calibration, representing pre-reservoir, post-landscape change conditions, was  
550 applied to the 1900– 1960 period; thereafter, we assume modern flood control, and applied the  
551 modern calibration. Pre-1900 estimates used the calibration based on 1880s data, except for the  
552 Vancouver period (1850– 1868), which used the mid-20<sup>th</sup> century model because there was no  
553 19<sup>th</sup> century model. The validity of the composite modeled  $T_w$  is assessed, to the extent possible,  
554 through comparison with in-situ measurements (see Results).

555 Uncertainty was assessed by evaluating the root-mean-square error (RSME) between the compo-  
556 site model estimate and measurements, and comparing against the RMSE found using climatol-  
557 ogy. The uncertainty in each temperature estimate was assessed using a Monte Carlo approach.  
558 Two thousand possible ensembles of the model coefficients were created, under the assumption  
559 that coefficient uncertainty was normally distributed. The 95<sup>th</sup> percentile of the resulting spread  
560 of solutions is reported.

## 561 3.0 Results and Discussion

### 562 3.1 Model Assessment

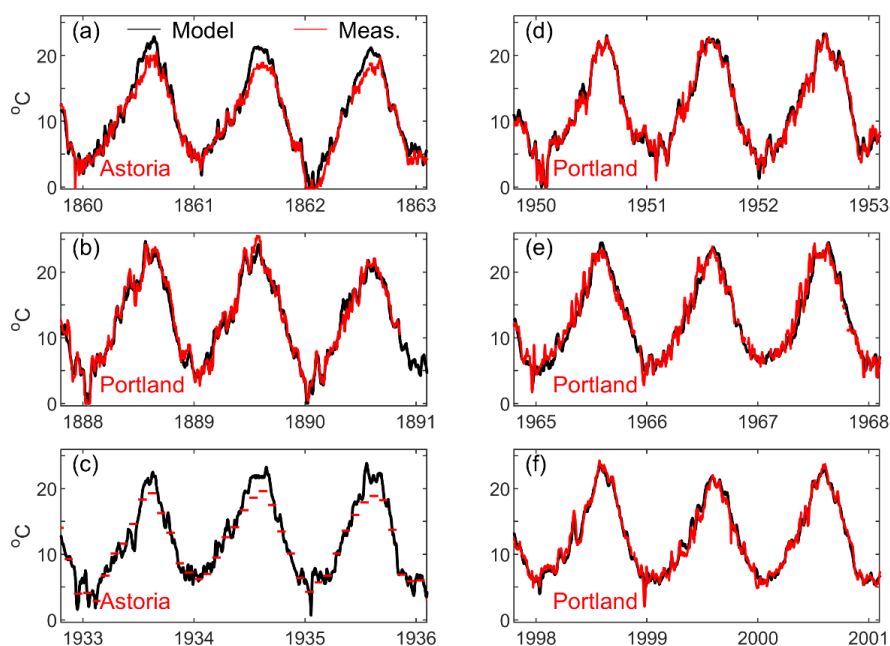
563 Time-series comparisons of water temperature (Figure 4) and statistical evaluations (Table 2)  
564 confirm that the statistical model reproduces reasonably well year-to-year differences in  $T_w$  and  
565 weekly-monthly perturbations caused by persistent warm/cold weather. Some synoptic scale  
566 events of less than a week are only partially captured, possibly because of factors not included in  
567 the model (such as cloud cover, wind, or depth changes due to backwater from the Columbia  
568 River; see also Wagner et al., 2011) and the tendency of statistical models to underestimate ex-  
569 tremes. The RMSE between the measured and modeled daily minimum  $T_w$  varies from 0.87 to  
570 1.1 °C for the annual model, with RMSE as low as 0.53 °C and 0.72 °C for the summertime and  
571 wintertime models, respectively (Table 2). Results are less good using Eola, a weather station  
572 which is located ~70km from Portland and may imperfectly represent local meteorological forc-  
573 ing. On a monthly averaged scale, RMSE varies from ~0.3 to 0.9 °C, with the best agreement  
574 obtained during the modern period and the summertime sub-models (Table 2).

575 Our statistical model results compare favorably with numerical models; the RMSE at Portland  
576 for a calibrated numerical model based on measurements from April through September 2002  
577 was 0.43 °C (Berger et al., 2004), compared to 0.52 °C for our model over the same period. Sim-  
578 ilarly, the model performs significantly better than estimates based on  $T_w$  climatology, which we  
579 calculate has a root-mean-square error (RMSE) of 1.86, 1.46, and 1.43 °C for the 1881– 1890,  
580 1941– 1952, and 2000– 2015 calibration periods, respectively. We conclude that the statistical  
581 model accurately represents the most important factors affecting  $T_w$ , as long as the underlying  
582 measurements driving the model are reasonably accurate.

583 Modeled  $T_w$  estimates based on different  $T_a$  data series (Table 2) compare well with each other,  
584 with similar averages and variability. During their period of overlap from 1940– 1973, modeled  
585 water temperatures are slightly larger (0.08 °C) using the airport model (1941A) than the down-  
586 town Portland model (1941D). Similarly, the Vancouver model (1941V model) is 0.02 °C lower  
587 than the airport model (1941A) between 1940 and 1965. For the same periods, the daily RMSE



588 between the 1941A model  $T_w$  and the 1941D and 1941V models is 0.29 °C and 0.32 °C, respec-  
589 tively. For the 1896– 1965 period, the 1941D and 1941V models show a mean difference of  
590 0.06 °C (Vancouver larger), and an RMSE of 0.37 °C. These observations provide an order of  
591 magnitude estimate of the aggregate influence of input data and model variability on uncertainty,  
592 whether caused by spatial variations in  $T_a$ , differences in the statistical coefficients, or instrumen-  
593 tal measurement uncertainty. The consistency and small RMSE between model results improves  
594 our confidence in results.

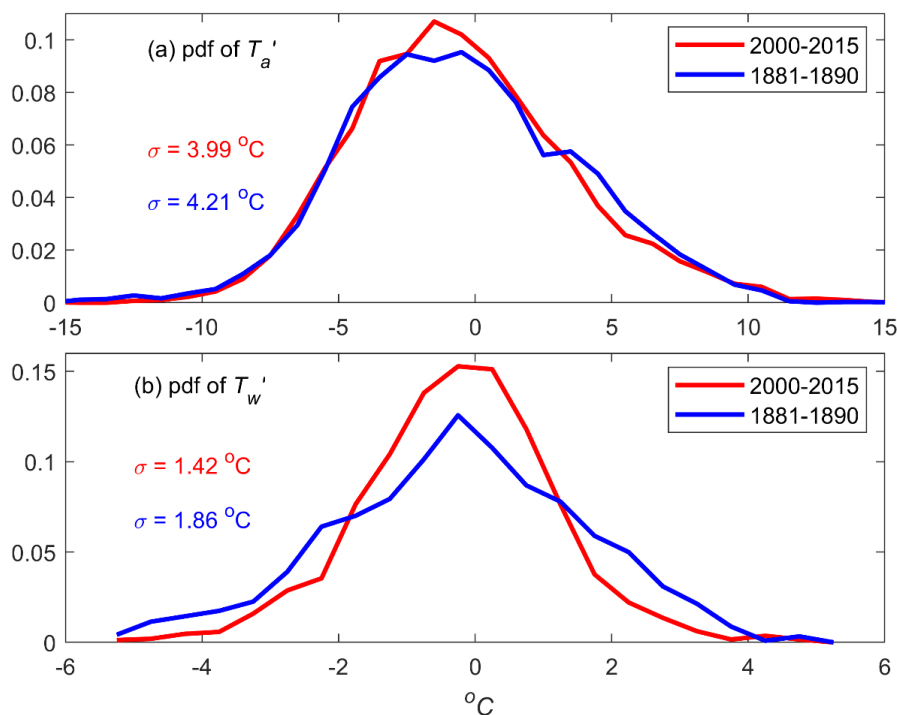


595

596 *Figure 4: Comparison of modeled and measured  $T_w$  for six periods of three years. The composite Port-*  
597 *land  $T_w$  is used in (b), (d), (e) and (f), while Astoria measurements are used in (a) and (c). Only monthly*  
598 *averages of  $T_w$  are available at Astoria from 1925 to 1940 and 1943– 1948 (see Table 1).*

599 One of the factors driving the larger RMSE in the historical model is the larger overall system  
600 variance measured for  $T_w$ . The typical distribution of  $T_a$  anomalies from the climatological mean  
601 has remained stationary between different time periods, and the standard deviation is nearly the  
602 same (within ~5%; Figure 5). However, between the 1880s and the 2000– 2015 period, the dis-  
603 tribution of measured  $T_w$  anomalies markedly contracted– , and the standard deviation decreased  
604 from 1.86 to 1.42 °C (Figure 5). Since the distribution of  $T_a$  anomalies remained similar, a likely  
605 explanation for the decreased variance in  $T_w$  is anthropogenic change to the local environment  
606 (e.g., flow regulation, landscape changes, system deepening), rather than changes in meteorolog-  
607 ical forcing (see below for further discussion).

608



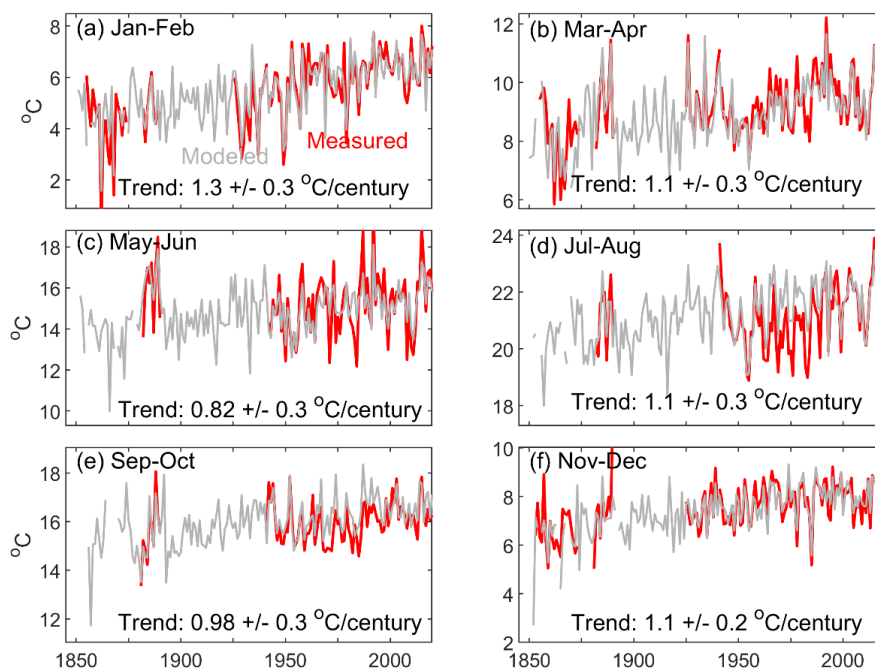
609

610 *Figure 5: The distribution of  $T_a$  and  $T_w$  around the 30d climatological mean for the 1881– 1890 and*  
611 *2000– 2015 periods.*

612

### 613 3.2 Water Temperature Changes in lower Willamette

614 Model results and measurements show that water temperatures have increased steadily since the  
615 1800s. Increases are observed at all times of the year (Figure 6), leading to an increase in annu-  
616 ally averaged  $T_w$  of  $1.1 \pm 0.2^\circ\text{C}/\text{century}$  (Figure 7). The largest increase occurred in winter; dur-  
617 ing January– February, the trend in average  $T_w$  is  $1.3 \pm 0.3^\circ\text{C}/\text{century}$  (Figure 6a). Similarly, the  
618 minimum annual temperature is increasing quickly, at  $1.8 \pm 0.5^\circ\text{C}/\text{century}$  (Figure 7b). The  
619 smallest bi-monthly averaged trends occur in late spring, during May– June ( $0.82 \pm 0.3^\circ\text{C}/\text{cen-}$   
620  $\text{tury}$  trend; Figure 6d). Maximum summer temperatures are trending upwards at  $\sim 0.9 \pm 0.3$   
621  $^\circ\text{C}/\text{century}$  (Figure 7c), smaller than the annual average. Overall, model results (grey) track avail-  
622 able in-situ measurements (red) well, except for some months during periods of lesser data qual-  
623 ity in the 1960s– 1970s (Figure 6 & 7). Therefore, modeled and measured trends are consistent,  
624 increasing confidence in results.



625

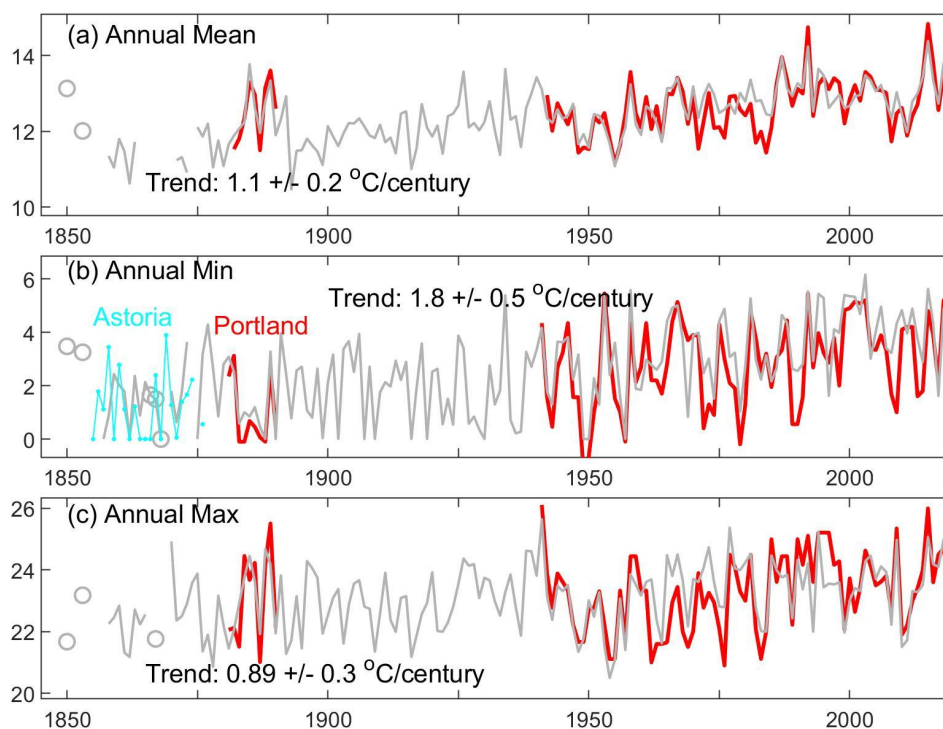
626 *Figure 6: Seasonal trends in water level, averaged over two month water periods. A correlation is found*  
627 *between measurements (red) and model results (grey). Trends and 95% confidence interval based on a*  
628 *linear regression to model results, 1850–2020. November–April data from 1854–1876 from Astoria, Or-*  
629 *egon (see Talke et al., 2020). Note different limits on the y-axis.*

630 No single event or individual system perturbation appears to be causing trends, as there are no  
631 step-function changes or inflection points in  $T_w$  trends (Figure 6 & 7). Instead, an upwards ten-  
632 dency in  $T_w$  is interspersed by large year-to-year variability. In the modern system, the largest in-  
633 terannual variation occurs during the spring period (May–June), with swings of  $\sim 5^\circ\text{C}$  observed  
634 between years (Figure 6). The late summer and autumn season (September–December) is least  
635 variable (order  $\sim 2^\circ\text{C}$  variability between years). Historically, greater year-to-year fluctuations  
636 occurred in both measurements and model results, particularly during the cooler half of the year  
637 (November–April). Cool-season measurements at Astoria (1854–1876) between November and  
638 April confirm this variability, and track modeled results despite its location on the Columbia  
639 River (see e.g. Figure 4a and 4c). The correspondence occurs because during late fall and winter,  
640 proportionally more water in the lower Columbia is sourced from coastal tributaries, especially  
641 the Willemette, than during other times of year (see Naik and Jay, 2011 and Hudson et al., 2017).

642 Both climatic factors and system changes drive the reduction in interannual variability in  $T_w$ .  
643 Storage reservoirs, with a large thermal inertia, are one factor (see section 3.3). The change from  
644 a multi-braided, shallow channel to a single, deeper channel is also likely influential. Another  
645 reason for historical  $T_w$  variability in winter was the occasional occurrence of deep freezes that



646 no longer occur. During the 1861–62 and 1867–1868 winters, for example, air temperatures re-  
647 mained below 0 °C for 32 and 31 days, respectively, and newspapers recorded ice-skating on the  
648 lower Willamette River. Navigation in Portland Harbor was halted or hindered by ice from New  
649 Year’s Day until mid-March, 1862. No 20<sup>th</sup> century winter matched the duration or severity of  
650 these events, though 18–19 freezing days (maximum below 0 °C) were recorded in 1915–16,  
651 1929–30, and 1949–50. In 1979, air temperatures remained below 0 °C for a total of 14 days;  
652 since 1980, no winter has produced more than 9 sub-freezing days. Because some historical win-  
653 ters were mild (e.g., only one freezing day was recorded in 1862–1863), historical water temper-  
654 atures in winter were much more variable than today.



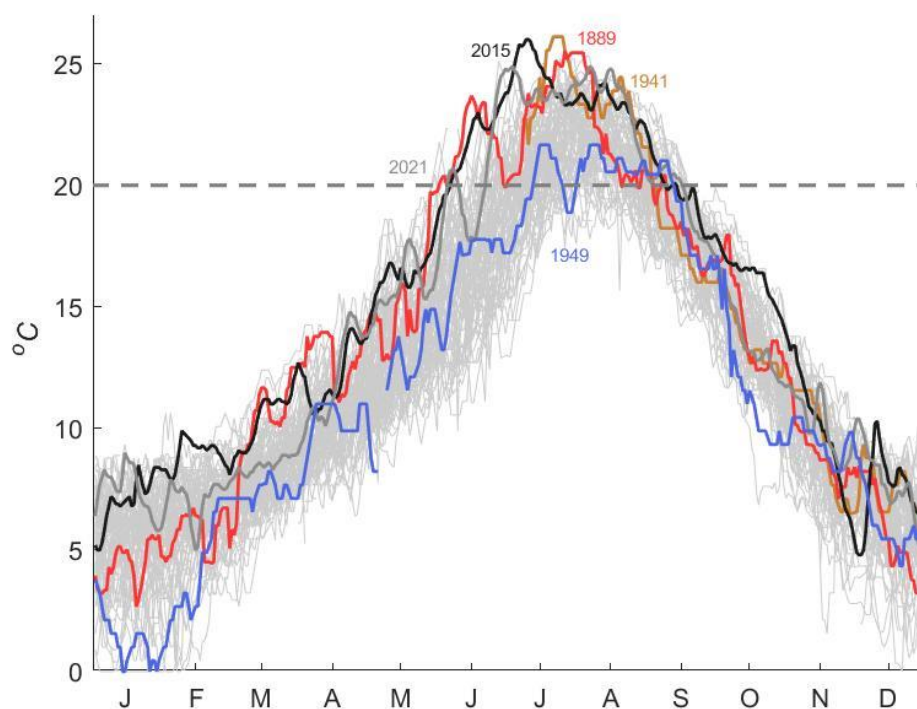
655

656 *Figure 7: Time rate of change of annual mean, annual minimum, and annual maximum  $T_w$ . Grey de-*  
657 *notes model data, red denotes data from Portland region, and cyan denotes  $T_w$  measurements in Astoria*  
658 *(annual minimum only). The trend is calculated by regression fit to the 1850–2015 period. Evaluation is*  
659 *based on daily minimum  $T_w$  (see section 2). Years in the 1850s and 1860s without sufficient model data*  
660 *are excluded.*

661 Results suggest that  $T_w$  has always exceeded a threshold of 20 °C during summer for ~15–90  
662 days, even during the 1800s (Figures 4, 7c, 8 and 9). A spaghetti plot of all available in-situ data  
663 shows that most  $T_w$  measurements exceeded the 20 °C threshold in July and August (Figure 8).



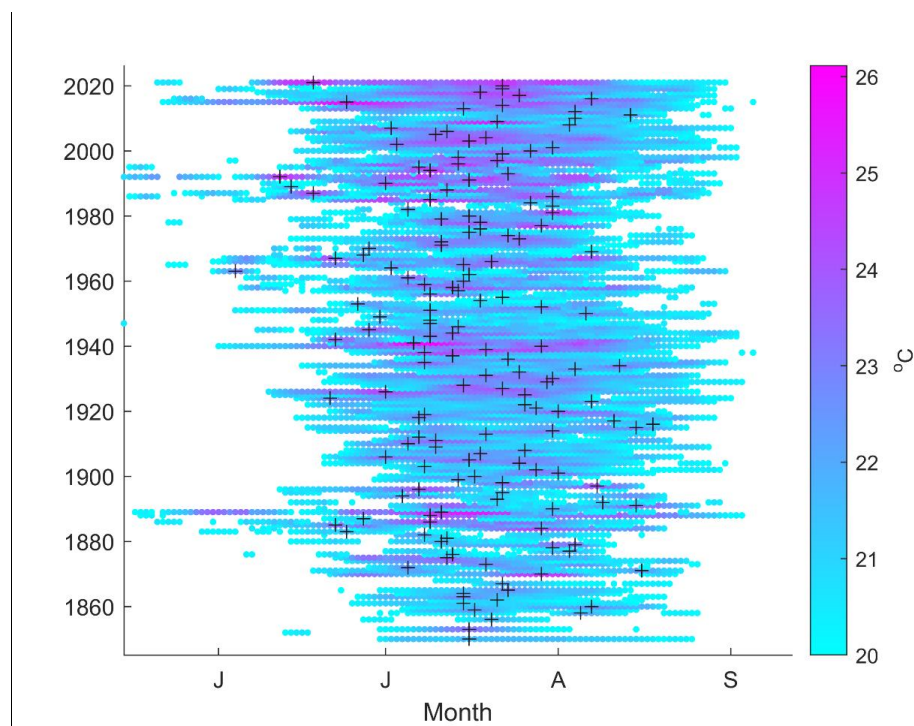
664 Peak temperatures typically occur during July or August, with no trend in timing observed (Fig-  
665 ure 8, 9). The timing meteorological heat waves within a summer—which appears to be ran-  
666 dom—drives the timing of the peak. During some cool summers historically (e.g., 1949; see Fig-  
667 ure 8), temperatures sometimes temporarily dipped below 20 °C during summer, and remained  
668 above the threshold for less than 2 months. In other years,  $T_w$  reaches a peak of 25–26 °C, and  
669 water temperatures remain above the biologically important 20 °C threshold from June to Sep-  
670 tember. During the hot, low river discharge summers of 1889 and 2015 (Figure 8), water temper-  
671 atures exceeded 20 °C for 91 and 95 days, respectively. The biggest difference, in line with other  
672 observations, is that  $T_w$  was more variable during the summer of 1889 than in 2015.



673

674 *Figure 8: Spaghetti plot of all measured  $T_w$  data from between 1881–1890 and 1941–2021. Five years*  
675 *(1889, 1941, 1949, 2015, and 2021) are colored as labeled. Time is labeled at the midpoint of each*  
676 *month.*



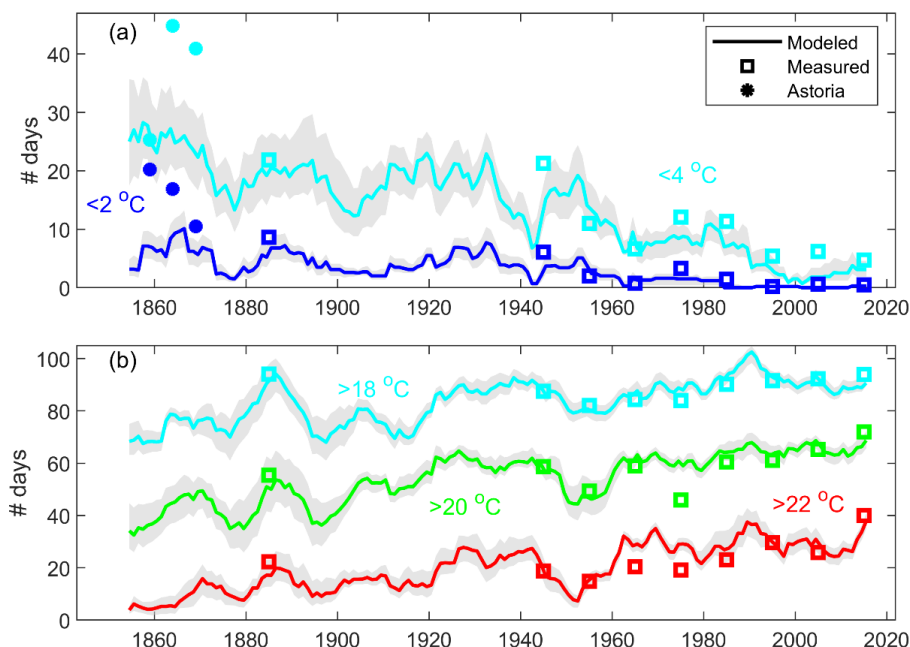


677

678 *Figure 9: Summertime  $T_w$  values in the Willamette River that exceed a threshold of 20 °C, from 1850 to*  
679 *2021. The instrumental record is used between 1881 and 1890 and 1941 to 2021, and the remainder is*  
680 *infilled with modeled  $T_w$ . Crosses denote the time of the peak annual  $T_w$ . Missing air temperature data*  
681 *precluded peak estimates for 1851–1852, 1854–1855, 1857, 1866, and 1868–1869 (see supplemental*  
682 *data). Time is labeled at the midpoint of each month.*

683 Summers with persistently elevated temperatures occur more often today, even though warm wa-  
684 ters occurred in some historical years (Figures 8 & 9). Between 1881–1890, measurements  
685 show that the 7-day average temperature exceeded the effective regulatory limit of 20.3°C (see  
686 Introduction) between 11–80 days, with an average of 42 days. For the 2000–2021 period, the  
687 range was 35–92 days of exceedances, with an average of 63 days (2 months). The more con-  
688 sistent warm summer water temperatures help explain the observed upward trend in  $T_w$  (Figure  
689 7). Interannual variability has also decreased, due in part to decreased sensitivity to synoptic  
690 (weather) related changes. Evaluated using a 10 year-average, the number of days per year that  
691 exceed 20 °C increased by roughly ~50% between 1850 and 2020, from around 40 d yr<sup>-1</sup> to more  
692 than 60 d yr<sup>-1</sup> (Figure 10), an increase of ~20 d. The threshold of 22 °C was exceeded relatively  
693 rarely in the 1800s (<5 days per year), but is now exceeded nearly 40 days per year. Before  
694 about 1960, there was more variability between decades than at present.

695 The number of cold-water days in winter has declined precipitously as overall temperatures have  
696 warmed (Figure 10a). Water temperatures are now rarely below 4 °C, compared to about 25 d



697

698 *Figure 10: Comparison of the modeled and measured number of days per year from 1850 to 2020 that*  
699  *$T_w$  is (a) below a threshold of  $2^{\circ}\text{C}$  and  $4^{\circ}\text{C}$  and (b) above thresholds of  $18^{\circ}\text{C}$ ,  $20^{\circ}\text{C}$ , and  $22^{\circ}\text{C}$ . Square sym-*  
700 *bol symbols denote the 10-year average based on measurements, while the solid line is a running 10 year aver-*  
701 *age of modeled  $T_w$ . Measurements based primarily on bias corrected upstream gauges (1962, 1983–*  
702 *1984) are excluded. Grey shading is the 95% confidence interval, based on resampling model coefficients*  
703 *using a Monte-Carlo based technique. Wintertime measurements from Astoria (1854– 1876) included in*  
704 *(a).*

705 per year in the mid-1800s. Similarly, near freezing temperatures (below  $2^{\circ}\text{C}$ ) were common in  
706 the 1800s (up to  $10\text{ d yr}^{-1}$ ), but almost never occur now. While an increase in winter water temper-  
707 atures has received much less attention than summer-time trends, this shift is also ecologically  
708 important (e.g., Webb & Weber, 1993; Caissie, 2006). For example, cold water events and win-  
709 tertime conditions influence the survivability and recruitment of fish by altering their biotic inter-  
710 actions, habitat use, physical condition, feeding rates, and community structure (see reviews by  
711 Hurst 2007; Brown et al., 2011; Weber et al., 2013). It is also possible that historical wintertime  
712 conditions, such as the deep freezes discussed above, provided some protection against non-na-  
713 tive plants and fauna that thrive in warmer waters.

### 714 3.3 Interpretation of water temperature changes

715 In general, seasonal patterns of measured  $T_w$  and shifts between 19<sup>th</sup> and 21<sup>st</sup> century data are  
716 consistent with measurements of  $T_a$ , with some slight variations in timing and magnitude (Figure  
717 11). Measurements in Portland indicate that the daily maximum air temperatures ( $T_a$ ) increased



718 by 1.3 °C between the 1875– 1904 and 1991– 2020 periods (Figure 11b), consistent with warm-  
719 ing trends of 0.5– 2 °C per century at 100+ stations throughout the Pacific Northwest (Mote et  
720 al., 2003) and an average increase of ~1.1 °C since 1900 (Mote et al., 2019). The smallest in-  
721 creases in Portland  $T_a$  occur in spring (April– June) and in late fall (November– December), and  
722 the largest occur in January– February and July– October, again consistent with  $T_a$  trends in the  
723 Maritime Pacific Northwest (Mote, 2003). Within Portland, the large summertime increase may  
724 be influenced by the urban heat Island effect (e.g., Voelkel et al., 2018). However, the city has  
725 been relatively urbanized (cleared of forest) since the beginning of the time series, and  $T_a$  mea-  
726 surements have primarily occurred by either the Willamette or Columbia River, both reasons that  
727 changes in temperature bias caused by infrastructure may be relatively small. Moreover, the dis-  
728 tribution of air temperatures around the climatological mean has remained virtually unchanged  
729 (Figure 5). Given the long history of Portland and later the Airport as the primary regional meas-  
730 urement station, and the consistency of trends with the regional average (e.g., Mote et al., 2019),  
731 we conclude that the  $T_a$  measurements are reasonably representative of regional climate patterns.

732 Average air temperatures during the 1881– 1890 calibration period (during the Signal Service  $T_w$   
733 measurements) are only 0.4 °C cooler than the 2000– 2015 calibration period (Figure 11d), mark-  
734 edly lower than the 1.3 °C difference between the 30y climatological averages (Figure 11b). A  
735 possible reason is that pre-1888 measurements may not have been properly sheltered (Mote  
736 2003). However, comparison with  $T_w$  measurements (compare Figure 11c with 11e) suggests  
737 that air and water temperature patterns during this decade were similar and warmer than previous  
738 and subsequent decades. For example, both springtime  $T_a$  and  $T_w$  measurements in the 1880s  
739 were higher than instrumental measurements from the 2000– 2015 period. The correspondence  
740 between  $T_a$  and  $T_w$  measurements in the 1880s increases confidence that measurements indicate a  
741 real climate signal, possibly caused by decadal fluctuations in climate (e.g., Peterson & Kinkel,  
742 2001), rather than an instrumental artifact.

743

### 744 3.3.1 Causes of $T_w$ Change

745

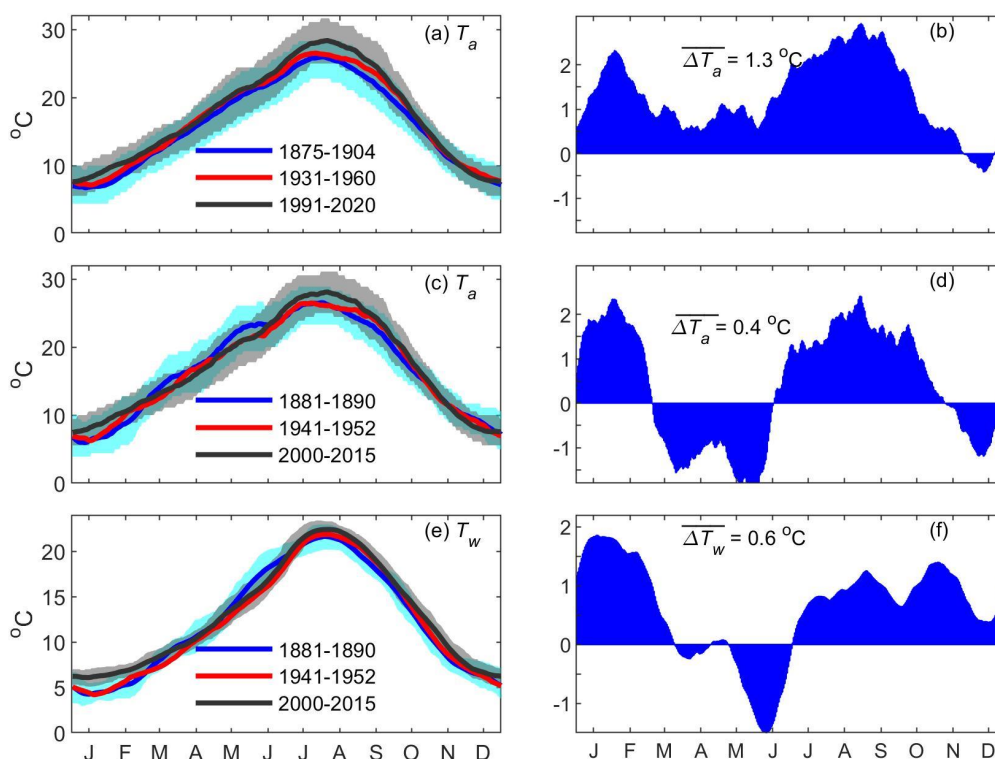
746 We next approximate the magnitude of factors causing  $T_w$  change using a series of sensitivity  
747 studies. These experiments provide an order-of-magnitude assessment of how sensitive the sys-  
748 tem is to changed coefficients or input data. We evaluate:

749

- 750 1. Integrated system changes. By applying the same input data to models from different  
751 time periods, we explore how the system response has changed to the same perturbations.  
752 River flow and  $T_a$  data from 2000– 2020 are used.
- 753 2. The effects of climate change. The climatological  $T_a$  increase since the 19th century in  
754 Portland is applied (Figure 11b), while river flow and the statistical model are kept the  
755 same.
- 756 3. The effect of water resources management. The change in the river hydrograph (Figure  
757 2a) is applied, with the system coefficients and  $T_a$  held constant.



758



759

760 *Figure 11:  $T_a$  and  $T_w$  climatology in Portland (a,c,e) and the difference between the modern (1991– 2020)*  
761 *and historical period (1881– 1890) in (b,d,e). Climatology is determined using a 30d moving average;*  
762 *shading denotes the 25<sup>th</sup> and 75<sup>th</sup> percentile of the measurements. A 30 year average is used in (a); the*  
763 *time periods for (c) and (e) are determined by the time period used to calibrate the  $T_w$  model. The tick*  
764 *marks on the x-axis denote the middle of each month. The average  $T_w$  difference between the modern*  
765 *and earliest period is provided in (b,d,e).*

766 Model results confirm that changes in  $T_a$  (driven by climate change) are the most significant fac-  
767 tor in long-term increases in  $T_w$ , with system changes an additional important contributor during  
768 the cool season (Figure 12). Seasonally, changes to  $T_a$  between the 1875– 1904 and 1991– 2020  
769 periods dominate the modeled trends in  $T_w$  during summer and early fall (July– October) and in  
770 late winter (Figure 12). Averaged over a year, a total increase in  $T_w$  of  $0.81 \pm 0.25$  °C is corre-  
771 lated to  $T_a$  changes. A maximum climate-induced change of  $\sim 1.7 \pm 0.3$  °C occurs in September.  
772 Climate shifts produce a lesser shift of 0.5– 0.6 °C increase in  $T_w$  in spring (late March to June),  
773 and little change occurs in December, consistent with air-temperature climatology (compare Fig-  
774 ure 11 and 12). Interestingly, uncertainty in the air temperature contribution is driven by the inher-  
775 ent 95% confidence in the air temperature climatology, which is  $\pm 0.22$  °C, rather than uncer-

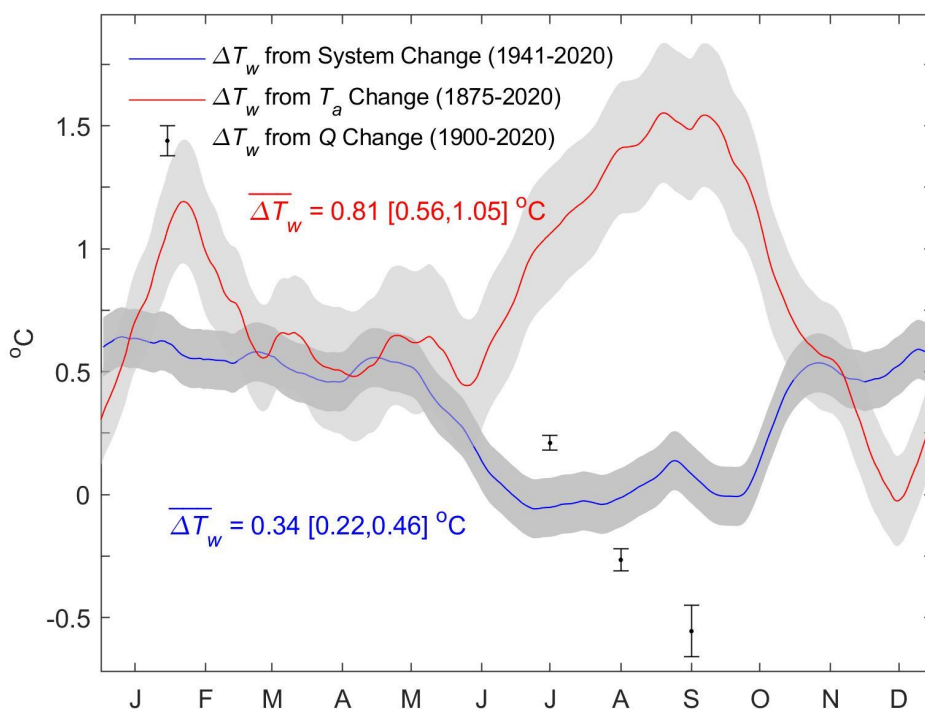


776 tainty in the model coefficients. Moreover, modeled  $T_w$  changes are robust to any small system-  
777 atic biases in  $T_a$ ; if the average change in  $T_a$  is reduced by  $0.5\text{ }^\circ\text{C}$ , the average  $T_w$  only decreases  
778 by  $\sim 0.3\text{ }^\circ\text{C}$ . Hence, we conclude that changes to the meteorological heat-balance (as represented  
779 by  $T_a$ ) are the major cause of increasing  $T_w$ . Climate models also suggest that future summertime  
780  $T_w$  in the Pacific Northwest will increase much more than other seasons, consistent with our re-  
781 sults (Ficklen et al., 2014).

782 System changes (as estimated by changing regression coefficients) between the 1940s and today  
783 cause a  $T_w$  increase of  $\sim 0.5\text{--}0.6\text{ }^\circ\text{C}$  from November–May, dropping to a statistically insignifi-  
784 cant amount from late June to early October. Averaged over a year, the total increase in  $T_w$   
785 caused by system change is  $0.34 \pm 0.12\text{ }^\circ\text{C}$ . The observed seasonal shifts are consistent with an  
786 increased thermal inertia caused by the reservoir system, as also discussed elsewhere (see e.g.  
787 Webb & Weber, 1993; Caissie 2006; Olden and Naiman, 2010). Effectively, heating or cooling  
788 from many months ago still influences  $T_w$  in the modern system, tending to elevate wintertime  
789 and depress summertime temperatures (see discussion for other influences). In the statistical  
790 model, we find that monthly averaged  $T_a$  exerts a statistical influence on  $T_w$  for 4 months, com-  
791 pared to 3 months historically (not shown). The coefficient magnitudes at 2–4 months lag are  
792 also larger today, at  $\sim 0.0025\text{ }^\circ\text{T}_w/\text{ }^\circ\text{T}_a$  per day (modern) vs.  $\sim 0.0017\text{ }^\circ\text{T}_w/\text{ }^\circ\text{T}_a$  per day (1940s; an-  
793 nual model). The other significant change in the modern model is a lessened sensitivity to syn-  
794 optic weather patterns, as observed by smaller coefficients at  $<7$  days lag (Figure 3) and less var-  
795 iance (Figure 5). Both the decreased sensitivity and the longer system memory in the modern  
796 system affect the modeled  $T_w$ , leading to the changed pattern of  $T_w$  responses to atmospheric  
797 forcing.

798 Changes in average river flow exert a minor influence on annually averaged  $T_w$ , but are im-  
799 portant during late summer. During July, a slight increase in  $T_w$  is observed from changed river  
800 flow. In August and especially September, the decrease in  $T_w$  caused by increased flow releases,  
801  $-0.27\text{ }^\circ\text{C}$  and  $-0.56\text{ }^\circ\text{C}$  are significant. Thus, the release of water from reservoirs late in the sum-  
802 mer counteracts, to some extent, the effects of increased air temperatures. During other times of  
803 year, no statistically significant modeled correlation between  $Q$  and  $T_w$  was found, likely because  
804 the average  $T_w$  gradient in the mainstem Willamette River is small (Figure 2b). While river flow  
805 may be important in winter during times of large positive or negative temperature gradients,  
806 these changes are likely transient and a process-based model would be required to capture it.  
807 The net effect of summertime changes in river flow on the annual average is small: A total de-  
808 crease in annually averaged  $T_w$  of  $\sim 0.05\text{ }^\circ\text{C}$  is estimated.

809



810

811 *Figure 12: Estimated  $T_w$  changes caused by  $T_a$  (climate change), system changes (i.e., differences be-*  
 812 *tween the parameters of the modern and historic models), and discharge changes (July– September). A*  
 813 *positive value indicates an increase over time. System changes are based on taking the difference in esti-*  
 814 *estimated  $T_w$  obtained over the 2000– 2020 time period using the 1940s era model (model 1941A) and the*  
 815 *modern era model (model 2000A). The influence of increased solar heating (climate change) is estimated*  
 816 *by differencing the  $T_a$  and  $T_w$  values obtained with the 1941A model using the 1875– 1904 and 1991–*  
 817 *2020  $T_a$  climatologies (Figure 11). Shading includes the both the 95% uncertainty in the mean climatol-*  
 818 *ogy and the 95% uncertainty in the coefficients. The July– September change in monthly averaged  $T_w$*   
 819 *produced by discharge is obtained by comparing the pre-reservoir (1901– 1940) and the modern (1981–*  
 820 *2020) hydrographs (Figure 2a) into the statistical model, with  $T_a$  forcing held constant. The error bars de-*  
 821 *note the difference in the 1941A and 2000A model estimates.*

822

823 Overall, the sum of estimated temperature changes caused by climate, system, and water man-  
 824 agement changes since ~1900 ( $\sim 1.1 \pm 0.3$  °C; Figure 12) is consistent with the overall long-term  
 825 trends in  $T_w$  of  $1.1 \pm 0.2$  °C per century (Figure 7a). Thus, we conclude that ongoing climate  
 826 change is the primary cause of increased temperatures, with system changes an important con-  
 827 tributor. We note again that we cannot discern the influence of individual factors such as  
 828 changed shading, river depth, storage, or snow pack, nor can we assess coupled, nonlinear



829 changes. For example, changes to river flow may in part be caused by climate change, and altera-  
830 tions in  $T_a$  may in part be influenced by urbanization or deforestation. Nonetheless, the results  
831 provide insights into the causes of  $T_w$  change and why some parts of the year are subject to larger  
832 upward trends than others, over secular timescales.

## 833 4.0 Discussion

834 The observed annual trend in  $T_w$  of  $1.1 \pm 0.2$  °C/ century in the lower Willamette River is similar  
835 to the magnitude of change observed or estimated in the few studies available over similar time  
836 scales. For example, Moatar and Gailhard (2006) estimated a 0.8 °C increase in the Loire since  
837 1881, Webb and Noblis (2007) estimated a change of 1.4– 1.7 °C on Austrian rivers since ~1900,  
838 and Scott (2020) estimated a trend of 1.3 °C/ century for the nearby Columbia River over the past  
839 170 years (see also Scott et al., 2022). Similar to our results, studies also often highlight that the  
840 seasonal distribution of changes of  $T_w$  is unequal (e.g., Webb and Noblis, 2007). Consistent with  
841 our results, studies from the Pacific Northwest suggest that climate change is driving  $T_w$  trends  
842 over recent decades (Isaak et al., 2012). Future climate change will continue to drive trends,  
843 with the largest increases in summer (Caldwell et al., 2013; Ficklin et al., 2014). But, our results  
844 suggest that system changes have altered the response of  $T_w$  to climate change, and in particular  
845 extremes, as explored below.

846 Both measurements (e.g., Figure 5) and the statistical model coefficients for  $T_a$  (Figure 3) sug-  
847 gest that the sensitivity of  $T_w$  to short-term meteorological forcing has decreased over time. A  
848 major cause is the reservoir system, which is known to decrease  $T_w$  variability in the Willamette  
849 on 1– 8 day time scales (Steel and Lange, 2007). At short time lags of 0–5 days, historical model  
850 coefficients are as much as 2–3x larger than modern coefficients (Figure 3). Therefore, a histori-  
851 cal heat wave in  $T_a$  was likely to produce a larger change in  $T_w$  than today. Simultaneously, the  
852 integrated effect of weather during previous months is more important. At lags of > 2 weeks, co-  
853 efficient magnitudes are ~50% larger in the modern models than historically. Hence, the thermal  
854 memory of the system to  $T_a$  anomalies lasting a month or longer is larger. Thermal memory  
855 stems from storage effects, whether from the heat stored in reservoirs (Webb & Weber, 1993;  
856 Caissie, 2006; Olden & Naiman, 2010) or the cooling effects of snow melt and groundwater in  
857 summer, which together are the primary source of water during this period (Brooks et al., 2012).  
858 The net thermal memory has increased, providing a buffering effect that helps explain why both  
859 seasonal and interannual variations in  $T_w$  are less pronounced today.

860 We attribute the decreased sensitivity of  $T_w$  to short-term, synoptic weather patterns (< 1 week)  
861 to a system-wide increase in depth, caused by the reservoir system (Rounds, 2007,2010) and by  
862 channelization and depth increases in the river (Sedell & Froggatt, 1984; Gregory et al., 2002a)  
863 A larger depth  $d$  decreases the magnitude of the heating term ( $\frac{H}{\rho c_p d}$ ) in Equation (1), leading to  
864 smaller temperature change in the leading order balance  $\frac{\partial T_w}{\partial t} = \frac{H}{\rho c_p d}$ . This explains the decrease  
865 in model coefficients for small time lags (< 1 week). Reservoirs in the upper watershed increase  
866 the mean depth of the entire system, reducing the overall rate of temperature change but increas-  
867 ing heat storage capacity (Caissie, 2006). Similarly, the transition from a multi-braided stream to  
868 a dredged river with one primary channel also contributes to increased depth, to an unknown ex-  
869 tent. Gravel mining and dredging for the harbor may also have increased depths in the lower



870 Willamette (see e.g., Jay et al., 2011). These Portland-region depth increases may be offset by a  
871 decrease in backwater effects from the Columbia River, particularly in spring (Helaire et al.,  
872 2019).

873 The changing correlation structure (Figure 3) and the influence of increasing depth has implica-  
874 tions for how climate change effects are observed. At short time scales (<1 week), the decreased  
875 modern sensitivity to air temperature perturbations (Figure 3) implies that depth increases out-  
876 weigh altered  $H$  in the heating term. If the correlation structure had remained unchanged, a 1 °C  
877 step increase in  $T_a$  would result in a larger short-term perturbation than is currently observed.  
878 Hence,  $T_w$  in the modern system has become more resilient to extreme heat waves. The record  
879 breaking heat wave in July 2021, with a high  $T_a$  of 46.7 °C, did not cause a record  $T_w$ . Despite  
880 air temperatures exceeding the previous all-time high by ~5 °C, the daily minimum water tem-  
881 peratures peaked just over 24 °C, in part because the heat wave was shorter than other events.  
882 We conclude that water temperatures are now more influenced by climate-change induced  
883 changes to air temperature climatology and long-time scale patterns, rather than short-term ex-  
884 treme events.

885 Numerical, process based models run over a smaller time scale provide additional clues to the  
886 factors driving long-term changes. For example, non-reservoir anthropogenic factors were mod-  
887 eled to increase Willamette River water temperatures in Portland by  $0.3 \pm 0.05$  °C between June  
888 and October of 2001 (OR DEQ, 2006), primarily due to loss of shading (86%) and secondarily  
889 because of point-source discharges (e.g., from water treatment plants). The same CE2-Qual  
890 model determined a reduction of approximately 0.1 °C for each additional 100 m<sup>3</sup>/s of river flow-  
891 released into the lower Willamette. This is consistent with our modern statistical model, which  
892 suggests an influence of ~0.07 °C for each extra 100 m<sup>3</sup>/s of river flow, spread out over several  
893 months via the decorrelation structure (Figure 3d).

894 River flow effects on  $T_w$  are likely driven by the substantial positive summertime  $\frac{dT_w}{dx}$  (Figure  
895 2b) during July-September, but are also influenced by the increased velocity and depth caused by  
896 each incremental increase in discharge (see Equation 1). The large increase in September dis-  
897 charge (Figure 2) reduces temperatures by 0.56 °C, a larger amount than in August (Figure 12).  
898 In October, average  $\frac{dT_w}{dx}$  becomes small (Figure 2), and our approach is unable to find a statisti-  
899 cally significant influence of river discharge.

900 Interestingly, the overall system was less sensitive to river flow fluctuations in the 1940s (Figure  
901 3d), and no statistically significant effect was observed in the 1880s. The lack of correlation in  
902 the 1880s may simply reflect imperfect flow estimates (see Jay & Naik, 2011). Nonetheless, it is  
903 possible that the bottomland forests and braided river networks of the historical Willamette River  
904 greatly reduced  $\frac{dT_w}{dx}$ , velocity, and the advective heating term during summer (Equation 1), pro-  
905 ducing the observed lack of correlation. Mechanisms that might be influential include stream  
906 width changes (e.g., White et al., 2017) and cold groundwater discharges, which is known to oc-  
907 cur in off-main channel alcoves (e.g., Faulkner et al., 2020). During winter, the shallower histori-  
908 cal streams may have contributed to the freezing water temperatures observed during some years  
909 in the 19<sup>th</sup> century. A process-based retrospective model using historical bathymetry would be  
910 required to further investigate these conjectures, and determine the relative roles of geomorphic  
911 change, ecological change, and the reservoir system on  $T_w$ .





912 Since spring  $T_a$  values are less changed than summer values (Figure 11), less extra heat is input  
913 at the beginning of the warm season, and warm  $T_w$  is not biased early in the modern record. In  
914 the late summer, reservoir releases are tamping  $T_w$  values downwards (Figure 12).

915 The increase in the number of days that temperatures exceed a threshold has been observed in  
916 other river systems (e.g., Markovic et al., 2013) and is projected to continue in the Pacific North-  
917 west (Mantua, 2010). Our observations show that the rate of change is threshold dependent, and  
918 slows as the accumulated number of days above a threshold becomes large. Therefore, the num-  
919 ber of days over 20 °C (which is already large) is increasing less quickly than the number of 22  
920 °C days, which occur primarily during mid-summer (Figure 9). Effectively, exceedences of  
921 lower thresholds like 18 °C and 20 °C are limited by spring and fall, when temperatures change  
922 quickly. Conversely, in winter, the largest rates of change are observed for larger levels of ex-  
923 ceedance; hence, the number of cold-water days below 4 °C is decreasing faster than those below  
924 2 °C. Average temperatures in Jan-Feb, the period with the coldest temperatures, have increased  
925 from ~0-6 degrees to 5-8 degrees (Figure 6a). Hence, both the decreased spread in temperatures  
926 (Figure 5) and the increased mean drive the large change in the number of days below 4 °C.

927 Compared to historical norms, water temperatures today exhibit less variability, both day-to-day  
928 and between the maximum and minimum (both climatology and daily extrema). A result is that  
929 *temporal refugia*—which we define as time periods in which water temperatures temporarily dip  
930 below biologically important thresholds such as 18 °C or 20 °C—are becoming less frequent (see  
931 Figure 9,10). Hence, while the management practice of selectively releasing river water is suc-  
932 cessfully reducing average temperatures in late summer (Figure 12), it may not be addressing the  
933 decrease in variance (e.g., Figure 5) caused by system changes. Because some migrating fish  
934 such as steelhead delay migration during warm periods by weeks or months, likely causing in-  
935 creased mortality (e.g., Siegel et al., 2021), the reduced temporal refugia are important to con-  
936 sider (see also Steel et al., 2012). At Portland,  $T_w$  exceeds—and has done so throughout the pe-  
937 riod of record—biologically important thresholds during some part of every year. However, the  
938 more consistently warm temperatures during summer and the shoulder seasons—as observed by  
939 the increase in the time over 18 °C and 20 °C—likely creates a thermal barrier that has implica-  
940 tions for salmon migration (see e.g., Notch et al., 2020).

## 941 5.0 Conclusion

942 In this contribution, we found, digitized, produced, and quality controlled a long  $T_w$  record  
943 (1881– 1890, 1941– 2021) for the lower Willamette River in Portland, Oregon. The in-situ  
944 measurements enabled the development of statistical  $T_w$  models based on the 1880s, 1940s, and  
945 modern time periods. Subsequently, estimates of daily minimum  $T_w$  for the years 1850– 2021  
946 are produced using daily measurements of  $T_a$  and river discharge. A good comparison between  
947 measurements and models is observed (Table 2), including cool season water temperature meas-  
948 urements (November – April) in the Columbia River Estuary from 1854– 1876.

949 Water temperatures are increasing throughout the year (average trend of  $1.1 \pm 0.2$  °C/ century),  
950 with the largest trends observed in winter. As a result, the number of cold water days per year is  
951 precipitously declining, while the number of days above 20 °C has increased by an average of  
952  $\sim 20$  d yr<sup>-1</sup> (Figure 10). The primary cause of changed  $T_w$  since ~1900 is climate change (0.84  
953 °C), followed by system changes such as the building of reservoirs, loss of shading, and other



954 landscape alterations (0.34 °C; Figure 12). Changes and reductions in flow have a generally  
955 smaller influence. Because of a larger heat capacity and greater system depth, the day-to-day var-  
956 iability in  $T_w$  has decreased (e.g., Figure 5). Even though average temperatures in summer are  
957 now larger, peak temperatures have changed less. Hence, warm summers marked by low river  
958 flow produced similar peak temperatures in 1889, 1941, and 2015 (Figure 9), and a truly extreme  
959 heat wave in 2021 did not produce record water temperatures, possibly because of its short dura-  
960 tion. The relative suppression of peak  $T_w$  has been bought at the expense of daily and interannual  
961 variability; during most times of the year, but particularly in winter, there is less day-to-day vari-  
962 ation than in the 19<sup>th</sup> century. Climatic induced disturbance events such as freezing rarely occur  
963 anymore. Similarly, temporal refugia—time periods in which  $T_w$  dips below biologically im-  
964 portant thresholds—have also decreased (Figures 9 & 10). These system changes may pose a  
965 grave threat to endemic species, should climate-induced changes in  $T_w$  continue.

966

## 967 Data Availability

968 The water temperature data used in the research is available upon request, and will be uploaded  
969 to a data repository upon acceptance of the manuscript. Meteorological data are available from  
970 the National Centers for Environmental Information (<https://www.ncei.noaa.gov/>). Pre-1890  
971 Vancouver and Portland records were also obtained from the Midwestern Regional Climate Cen-  
972 ter ([https://mrcc.illinois.edu/data\\_serv/cdmp/cdmp.jsp](https://mrcc.illinois.edu/data_serv/cdmp/cdmp.jsp)). River flow records are obtained from  
973 the US Geological Survey and the sources described in section 2.

## 974 Author Contribution

975 SAT found and processed archival data, developed the statistical model, analyzed results, pro-  
976 duced figures, and was primary lead on drafting the paper. DAJ developed an earlier version of  
977 the model and assisted with interpretation and paper development. HLD assisted with interpreta-  
978 tion and paper drafts, and helped secure funding.

## 979 Competing Interests

980 The authors declare that they have no conflict of interest

## 981 Acknowledgements

982 Funding was provided by Bonneville Power Administration, under Project No. 2002-077-00 with  
983 the Pacific Northwest National Laboratory, and by the US National Science Foundation, CA-  
984 REER Award 1455350 and NSF project 2013280. Margaret McKeon is thanked for her help de-  
985 fining the watershed boundaries in Figure 1, and students at Portland State University are  
986 thanked for helping to digitize and quality assure the 1854-1876, 1881-1890, and 1941-1961 wa-  
987 ter temperature records used in this study.

988



## 989 References

- 990  
991 Al-bahadily, A.: Long Term Changes to the Lower Columbia River Estuary (LCRE) Hydrody-  
992 namics and Salinity Patterns. PhD thesis. Portland State University, doi:  
993 10.15760/etd.7357, 2020.
- 994 Al-Murib, M. D., Wells, S. A., and Talke, S. A.: Integrating Landsat TM/ETM+ and numerical  
995 modeling to estimate water temperature in the Tigris River under future climate and man-  
996 agement scenarios. *Water*, 11(5), 892, doi.org/10.3390/w11050892, 2019.
- 997 Angilletta M.J., Steel E.A., Bartz K.K., Kingsolver J.G.,Scheurell M.D., Beckman B.R.,  
998 and Crozier L.G.: Big dams and salmon evolution: changes in thermal regimes and  
999 their potential evolutionary consequences. *Evolutionary Applications*,1, 286–299, doi:  
1000 10.1111/j.1752-4571.2008.00032.x, 2008.
- 1001 Annear, R., McKillip, M., Khan, S. J., Berger, C., and Wells, S.: Willamette Basin Temperature  
1002 TMDL Model: Boundary Conditions and Model Setup, Technical Report EWR-03-03,  
1003 Department of Civil and Environmental Engineering, Portland State University, Portland,  
1004 Oregon, 2003.
- 1005 Baker, J., Van Sickle, D., White, D.: Water Sources and Allocation. In: Willamette River Basin  
1006 Planning Atlas (D. Hulse, S. Gregory and J. Baker, Eds.), pp. 40–43. Oregon State Uni-  
1007 versity Press, Corvallis, 2002.
- 1008 Benyahya L., Caissie,D.,St-Hilaire, A., Ouarda, T.B.M.J., and B. Bobée.: A Review of statistical  
1009 water temperature models. *Canadian Water Resources Journal*. 32(3): 179-192,  
1010 doi.org/10.4296/cwrj3203179, 2007.
- 1011 Benner, P., and Sedell, J.: Upper Willamette River Landscape: A Historic Perspective. in *River*  
1012 *Quality : Dynamics and Restoration*. Ed. Antonius Laenen and David A. Dunnette. Boca  
1013 Raton: CRC/Lewis, 23-46, 1997.
- 1014 Berger, C., McKillip, M.L., Annear, R.L., Khan, S.J., and Wells, S.A.: Willamette Basin Tem-  
1015 perature TDML Model: Model Calibration. Portland State University, Department of  
1016 Civil and Environmental Engineering. Technical Report EWR-02-04, 2004.
- 1017 Branscomb,A., Goicochea J., and Richmond, M.: Stream Network. In: Willamette River Basin  
1018 Planning Atlas (D. Hulse, S. Gregory and J. Baker, Eds.), pp. 16-17. Oregon State Uni-  
1019 versity Press, Corvallis, 2002.
- 1020 Brooks, J. R., Wigington, P. J., Phillips, D. L., Comeleo, R., and Coulombe, R.: Willamette  
1021 River Basin surface water isoscape ( $\delta$  18O and  $\delta$  2H): temporal changes of source water  
1022 within the river, *Ecosphere*, 3, 39, doi:10.1890/ES11-00338.1, 2012.
- 1023 Brown, R. S., Hubert, W. A., and Daly, S. F.: A primer on winter, ice, and fish: what fisheries  
1024 biologists should know about winter ice processes and stream-dwelling fish. *Fisher-*  
1025 *ies*, 36(1), 8-26, doi.org/10.1577/03632415.2011.10389052, 2011.
- 1026 Bumbaco, K. A., Dello, K.D., and Bond, N.A.: History of Pacific Northwest Heat Waves: Syn-  
1027 optic Pattern and Trends. *Journal of Applied Meteorology and Climatology*,  
1028 DOI:10.1175/JAMC-D-12-094.1, 2013.
- 1029 Bottom, D., Baptista, A., Burke, J., Campbell, L., Casillas, E., Hinton, S., Jay, D.A., Lott, M. A.,  
1030 McCabe, G., McNatt, R., Ramirez, M., Roegner, G. C., Simenstad, C. A., Spilseth, S.,  
1031 Stamatou, L., Teel, D. and Zamon, J. E.: Estuarine habitat and juvenile salmon: Current  
1032 and historical linkages in the Lower Columbia River and estuary. Final report, 2002-



- 1033 2008. Report of the National Marine Fisheries Service to the U.S. Army Corps of Engi-  
1034 neers. Portland, Oregon. Available at <https://www.nwfsc.noaa.gov/publications/in->  
1035 [dex.cfm](https://www.nwfsc.noaa.gov/publications/index.cfm), 2011.
- 1036 Boyd, Robert, ed. *Indians, Fire, and the Land in the Pacific Northwest*: Corvallis: Oregon State  
1037 University Press, 1999.
- 1038 Caissie, D., El-Jabi, N. and St-Hilaire, A.: Stochastic Modelling of Water Temperatures in a  
1039 Small Stream Using Air to Water Relations. *Canadian Journal of Civil Engineering*, 25:  
1040 250–260, doi.org/10.1139/197-091, 1998.
- 1041 Caissie, D.: The thermal regime of rivers: a review. *Freshwater Biology*, 51: 1389-1406,  
1042 doi.org/10.1111/j.1365-2427.2006.01597.x, 2006.
- 1043 Caldwell, R.J., Gangopadhyay, S., Bountry, J., Lai, Y. and Elsner, M.M.: Statistical modeling of  
1044 daily and subdaily stream temperatures: Application to the Methow River Basin, Wash-  
1045 ington. *Water Resources Research*. 49: 4346 – 4361, doi.org/10.1002/wrcr.20353, 2013.
- 1046 Chang, H., and Jung, I. W.: Spatial and temporal changes in runoff caused by climate change in a  
1047 complex large river basin in Oregon. *Journal of Hydrology*, 388(3), 186-207,  
1048 doi.org/10.1016/j.jhydrol.2010.04.040, 2010.
- 1049 Christy, J.A. and Alverson, E.R., 2011. Historical vegetation of the Willamette Valley, Oregon,  
1050 circa 1850. *Northwest Science*, 85(2), pp.93-107.
- 1051 Crozier, L. G., Siegel, J. E., Wiesebron, L. E., Trujillo, E. M., Burke, B. J., Sandford, B. P., &  
1052 Widener, D. L.: Snake River sockeye and Chinook salmon in a changing climate: impli-  
1053 cations for upstream migration survival during recent extreme and future climates. *PloS*  
1054 *one*, 15(9), e0238886, doi.org/10.1371/journal.pone.0238886, 2020.
- 1055 Donato, M.M.: A Statistical Model for Estimating Stream Temperatures in the Salmon and  
1056 Clearwater River Basins, Central Idaho. US Geological Survey Water Resources Investi-  
1057 gations Report 2002-4195, 2002.
- 1058 Dugdale, S. J., Hannah, D. M., and Malcolm, I. A.: River temperature modelling: a review of  
1059 process-based approaches and future directions. *Earth Sci. Rev.* 175, 97–113. doi:  
1060 10.1016/j.earscirev.2017.10.009, 2017.
- 1061 Erickson, T. R., Stefan, H. G.: Linear air/water temperature correlation for streams during open  
1062 water periods. *Journal of Hydrologic Engineering*. 5(3): 317-321,  
1063 doi.org/10.1061/(ASCE)1084-0699(2000)5:3(317), 2000.
- 1064 Faulkner B.R., Brooks J.R., Keenan D.M., and Forshay K.J.: Temperature Decrease along  
1065 Hyporheic Pathlines in a Large River Riparian Zone. *Ecohydrology*. 1;13(1):1-10. doi:  
1066 10.1002/eco.2160. PMID: 32983317; PMCID: PMC7513865, 2020.
- 1067 Ficklin, D. L., Barnhart, B. L., Knouft, J. H., Stewart, I. T., Maurer, E. P., Letsinger, S. L. and  
1068 Whittaker, G. W.: Climate change and stream temperature projections in the Columbia  
1069 River basin: habitat implications of spatial variation in hydrologic drivers. *Hydrol. Earth*  
1070 *Syst. Sci.*, 18, 4897–4912, <https://doi.org/10.5194/hess-18-4897-2014>, 2014.
- 1071 Fischer, H.B., List, E.J., Koh, R.C.Y., Imberger, J., and Brooks, N.H.: *Mixing in inland and*  
1072 *coastal waters*. New York: Academic, 1979.
- 1073 Gregory, S., Ashkenas, L., Oetter, D., Minear, P., and Wildman, K.: Historical Willamette River  
1074 Channel Change. In: *Willamette River Basin Planning Atlas* (D. Hulse, S. Gregory and J.  
1075 Baker, Eds.), pp. 18-25. Oregon State University Press, Corvallis, 2002a.
- 1076 Gregory, S., Ashkenas, L., Oetter, D. Wildman, R., Minear, P., Jett, S., and Wildman, K.: Revet-  
1077 ments, In: *Willamette River Basin Planning Atlas* (D. Hulse, S. Gregory and J. Baker,  
1078 Eds.), pp. 32–33. Oregon State University Press, Corvallis, 2002b.



- 1079 Gregory, S., Ashkenas L., Jett, S., and Wildman, R.: Flood inundations/FEMA floodplains. In:  
1080 Willamette River Basin Planning Atlas (D. Hulse, S. Gregory and J. Baker, Eds.), pp. 28–  
1081 29. Oregon State University Press, Corvallis, 2002c.
- 1082 Gregory, S., Ashkenas L., Oetter, D., Minear, P., Wildman, K., Christy, J., Kolar, S., and Alver-  
1083 son, E.: Presettlement Vegetation ca. 1851. In: Willamette River Basin Planning Atlas  
1084 (D. Hulse, S. Gregory and J. Baker, Eds.), pp. 38–39. Oregon State University Press, Cor-  
1085 vallis, 2002d.
- 1086 Gregory, S., Ashkenas, L., Haggerty, P., Oetter, D. Wildman, K., Hulse, D., Branscomb, A. and  
1087 Van Sickle, J.: Riparian vegetation, In: Willamette River Basin Planning Atlas (D. Hulse,  
1088 S. Gregory and J. Baker, Eds.), pp. 40–43. Oregon State University Press, Corvallis,  
1089 2002e.
- 1090 Gregory, S.V., Frederick J. Swanson, W. Arthur McKee, Kenneth W. Cummins, An Ecosystem  
1091 Perspective of Riparian Zones: Focus on links between land and water, *BioScience*, Vol-  
1092 ume 41, Issue 8, Pages 540–551, <https://doi.org/10.2307/1311607>, 1991.
- 1093 Gregory, S., Wildman, R., Hulse, D., Ashkenas, L. and Boyer, K.: Historical changes in hydrology,  
1094 geomorphology, and floodplain vegetation of the Willamette River, Oregon. *River  
1095 Research and Applications*, 35(8), pp.1279-1290, 2019.
- 1096 Helaire, L.T., Talke, S.A., Jay, D. A. and Mahedy, D.: Historical changes in Lower Columbia  
1097 River and Estuary Floods and Tides. *Journal of Geophysical Research*, 124(11)  
1098 <https://doi.org/10.1029/2019JC015055>, 2019.
- 1099 Hudson, A.S., Talke, S.A., and Jay, D.A.: Using satellite observations to characterize the re-  
1100 sponse of estuary turbidity maxima to external forcing. *Estuaries and Coasts* 39(5) DOI  
1101 10.1007/s12237-016-0164-3, 2017
- 1102 Hurst, T. P.: Causes and consequences of winter mortality in fishes. *Journal of Fish Biol-*  
1103 *ogy*, 71(2), 315-345, [doi.org/10.1111/j.1095-8649.2007.01596.x](https://doi.org/10.1111/j.1095-8649.2007.01596.x), 2007.
- 1104 Jay, D.A., and Naik, P.: Distinguishing Human and Anthropogenic Influences on Hydrological  
1105 Disturbance Processes in the Columbia River, USA. *Hydrological Sciences Journal*.  
1106 56:7, 1186-1209, <https://doi.org/10.1080/02626667.2011.604324>, 2011.
- 1107 Jay, D. A., Leffler, K., and Degens, S.: Long-term evolution of Columbia River tides. *Journal of*  
1108 *waterway, port, coastal, and ocean engineering*, 137(4), 182-191,  
1109 [doi.org/10.1061/\(ASCE\)WW.1943-5460.0000082](https://doi.org/10.1061/(ASCE)WW.1943-5460.0000082), 2011.
- 1110 Johannessen, C.L., Davenport, W.A., Millet, A. and McWilliams, S.: The vegetation of the  
1111 Willamette valley 1. *Annals of the Association of American Geographers*, 61(2), pp.286-  
1112 302, 1971.
- 1113 Johnson S.L. and Jones J.A.: Stream temperature response to forest harvest and debris flows in  
1114 western Cascades, Oregon. *Canadian Journal of Fisheries and Aquatic Sciences*, 57  
1115 (Suppl. 2), 30–39, [doi.org/10.1139/cjfas-57-S2-30](https://doi.org/10.1139/cjfas-57-S2-30), 2000.
- 1116 Kaushal, S. S., Likens, G. E., Jaworski, N. A., Pace, M. L., Sides, A. M., Seekell, D., Belt, D.H.,  
1117 Secor, R.L., and Wingate, R. L.: Rising stream and river temperatures in the United  
1118 States. *Frontiers in Ecology and the Environment*, 8(9), 461-466,  
1119 [doi.org/10.1890/090037](https://doi.org/10.1890/090037), 2010.
- 1120 Landers D., Fernald A., Andrus C.: Off-channel Habitats. In: Willamette River Basin Planning  
1121 Atlas (D. Hulse, S. Gregory and J. Baker, Eds.), pp. 26-27. Oregon State University  
1122 Press, Corvallis, 2002.



- 1123 Lee, K.: Stream Velocity and Dispersion Characteristics Determined by Dye-Tracer Studies on  
1124 Selected Stream Reaches in the Willamette River Basin, Oregon. U.S. Geological Survey  
1125 Water-Resources Investigations Report 95–4078, 1995.
- 1126 Mantua, N., Tohver, I., and Hamlet, A.: Climate change impacts on streamflow extremes and  
1127 summertime stream temperature and their possible consequences for freshwater salmon  
1128 habitat in Washington State. *Climatic Change*, 102(1), 187–223, 2010.
- 1129 Markovic, D., Scharfenberger, U., Schmutz, S., Pletterbauer, F., and Wolter, C.: Variability and  
1130 alterations of water temperatures across the Elbe and Danube River Basins. *Climatic  
1131 Change* 119, 375–389, doi.org/10.1007/s10584-013-0725-4, 2013.
- 1132 Mayer, T.D.: Controls of summer stream temperature in the Pacific Northwest. *Journal of Hy-  
1133 drology*, 475, 323–335. <https://doi.org/10.1016/j.jhydrol.2012.10.012>, 2012.
- 1134 Monthly Weather Review (MWR): American Meteorological Society, Online ISSN: 1520-0493,  
1135 Volume 9 to 17, 1881–1889.
- 1136 Moore, A. M.: Correlation and analysis of water temperature data for Oregon Streams. United  
1137 States Geological Survey Water-Supply Paper 1818-K, 53 pages, 1967.
- 1138 Moore, A. M.: Water temperatures in the lower Columbia River. United States Geological Sur-  
1139 vey, Circular 551, doi.org/10.3133, 1968.
- 1140 Mote, P.W.: Trends in temperature and precipitation in the Pacific Northwest during the twenti-  
1141 eth century. Washington State University, 2003.
- 1142 Mote, P.W., Parson E. A., Hamlet, A. F., Keeton, W. S., Lettenmaier D., Mantua, N, Miles, E.  
1143 L., Peterson, D. W., Peterson, D. L, Slaughter, R., and Snover, A.K.: Preparing for Cli-  
1144 matic Change: The Water, Salmon, and Forests of the Pacific Northwest. *Climatic  
1145 Change* 61, no. 1-2, 45–88, doi.org/10.1023/A:1026302914358, 2003.
- 1146 Mote, P. W., and Salathé, E. P.: Future climate in the Pacific Northwest. *Climatic  
1147 change*, 102(1), 29–50, doi.org/10.1007/s10584-010-9848-z, 2010.
- 1148 Mote, P.W., Rupp, D.E., Li, S., Sharp, D.J., Otto, F., Uhe, P.F., Xiao, M., Lettenmaier, D.P.,  
1149 Cullen, H. and Allen, M. R.: Perspectives on the cause of exceptionally low 2015 snow-  
1150 pack in the western United States, *Geophysical Research Letters*, 43,  
1151 doi:10.1002/2016GLO69665, 2016.
- 1152 Mote, P. W., Li, S., Lettenmaier, D. P., Xiao, M., and Engel, R.: Dramatic declines in snowpack  
1153 in the western US. *Npj Climate and Atmospheric Science*, doi:10.1038/s41612-018-0012-  
1154 1, 2018.
- 1155 Mote, P.W., Abatzoglou, J., Dello, K.D., Hegewisch, K., and Rupp, D.E.: Fourth Oregon Cli-  
1156 mate Assessment Report. Oregon Climate Change Research Institute. [ocri.net/ocar4](http://ocri.net/ocar4);  
1157 accessed online February 4, 2019, 2019.
- 1158 Naik, P. K. and D. A. Jay.: Human and climate impacts on Columbia River hydrology and salm-  
1159 onids. *River Research and Applications*. 27: 1270–1276, DOI:10.1002/rra.1422, 2011.
- 1160 National Academies of Sciences, Engineering, and Medicine 2022. An Approach for Assessing  
1161 U.S. Gulf Coast Ecosystem Restoration: A Gulf Research Program Environmental Moni-  
1162 toring Report. Washington, DC: The National Academies Press.  
1163 <https://doi.org/10.17226/26335>
- 1164 Notch, J.J., McHuron, A.S., Michel, C.J., Cordoleani, F., Johnson M., Henderson, M.J. and Am-  
1165 mann, A.J.: Outmigration survival of wild Chinook salmon smolts through the Sacra-  
1166 mento River during historic drought and high water conditions. *Environ Biol  
1167 Fish* 103, 561–576. <https://doi.org/10.1007/s10641-020-00952-1>, 2020.



- 1168 Olden J. D. and R. J. Naiman.: Incorporating thermal regimes into environmental flows assess-  
1169 ments: modifying dam operations to restore freshwater ecosystem integrity. *Freshwater*  
1170 *Biology* 55: 86–107, doi.org/10.1111/j.1365-2427.2009.02179.x, 2010.
- 1171 Oregon Department of Environmental Quality (OR-DEQ): Willamette Basin TMDL and  
1172 WQMP. Chapter 4: Temperature-Mainstem TDML and subbasin Summary. Accessed  
1173 from <https://www.oregon.gov/deq/wq/tmdls/Pages/willamette2006.aspx>, accessed 2021-  
1174 08-21, 2006.
- 1175 Payne, S. K.: Dams. In: *Willamette River Basin Planning Atlas* (D. Hulse, S. Gregory and J.  
1176 Baker, Eds.), pp. 30-31. Oregon State University Press, Corvallis, 2002.
- 1177 Petersen, J. and Kitchell, J.: Climate regimes and water temperature changes in the Columbia  
1178 River: Bioenergetic implications for predators of juvenile salmon. *Canadian Journal of*  
1179 *Fisheries and Aquatic Sciences - CAN J FISHERIES AQUAT SCI.* 58. 1831-1841.  
1180 10.1139/cjfas-58-9-1831, 2001.
- 1181 Pohle I., Helliwell, R., Aube, C., Gibbs, S., Spencer, M. and Spezia, L.: Citizen science evidence  
1182 from the past century shows that Scottish rivers are warming. *Sci. Tot. Envr.*  
1183 10.1016/j.scitotenv.2018.12.325, 2019.
- 1184 Rounds, S.A.: Thermal effects of dams in the Willamette River basin, Oregon: U.S. Geological  
1185 Survey Scientific Investigations Report 2010-5153, 64 p, 2010.
- 1186 Rounds, S.A.: Temperature effects of point sources, riparian shading, and dam operations on the  
1187 Willamette River, Oregon: U.S. Geological Survey Scientific Investigations Report 2007-  
1188 5185, 34 p. (Also available at <http://pubs.usgs.gov/sir/2007/5185/>), 2007.
- 1189 Sedell, J.R. and Froggatt, J.L.: Importance of streamside forests to large rivers: The isolation of  
1190 the Willamette River, Oregon, USA, from its floodplain by snagging and streamside for-  
1191 est removal, *Internationale Verinigung fur Theoretische and Angewandte Limnologie*  
1192 *Verhandlungen (International Association for Theoretical and Applied Limnology)* 22,  
1193 1828–1834, 1984.
- 1194 Steel, E. A., and Lange, I. A.: Using wavelet analysis to detect changes in water temperature re-  
1195 gimes at multiple scales: Effects of multi-purpose dams in the Willamette River ba-  
1196 sin. *River Research and Applications*, 23(4), 351-359, doi.org/10.1002/rra.985, 2007.
- 1197 Steel, E. A., Tillotson, A., Larsen, D. A., Fullerton, A. H., Denton, K. P., & Beckman, B. R.: Be-  
1198 yond the mean: the role of variability in predicting ecological effects of stream tempera-  
1199 ture on salmon. *Ecosphere*, 3(11), 1-11, doi.org/10.1890/ES12-00255.1, 2012.
- 1200 Scott, M.H.: Statistical Modeling of Historical Daily Water Temperatures in the Lower Columbia  
1201 River. Masters Thesis, Portland State University, 2020.
- 1202 Scott, M.H., Talke, S.A., Jay, D.A. and Diefenderfer, H.: Warming of the Columbia River, 1853-  
1203 2018. Submitted to *Water Resources Research*, Submission 2022WR033330, 2022.
- 1204 Talke, S.A., Mahedy, A., Jay, D.A., Lau, P. Hilley, C., and Hudson, A.: Sea level, tidal and river  
1205 flow trends in the Lower Columbia River Estuary, 1853-present, *Journal of Geophysical*  
1206 *Research-Oceans.* <https://doi.org/10.1029/2019JC015656>, 2020.
- 1207 Taylor, J.E.: *Making Salmon: An Environmental History of the Northwest Fisheries Crisis.*  
1208 University of Washington Press, 488pp, 1999.
- 1209 Thilenius, J.F., 1968. The *Quercus garryana* forests of the Willamette valley, Oregon. *Ecology*,  
1210 49(6), pp.1124-1133.
- 1211 Thompson, P. R., Widlansky, M. J., Hamlington, B. D., Merrifield, M. A., Marra, J. J., Mitchum,  
1212 G. T., and Sweet, W.: Rapid increases and extreme months in projections of United



- 1213 States high-tide flooding. *Nature Climate Change*, 11(7), 584-590,  
1214 doi.org/10.1038/s41558-021-01077-8, 2021.
- 1215 U.S. Census: Statistics of The United States (Including Mortality, Property, &c.) in 1860; com-  
1216 piled from the original returns and being the final exhibit of the Eighth Census. Depart-  
1217 ment of the Interior, Washington D.C., Government Printing Office, 1866.
- 1218 USC&GS (US Coast and Geodetic Survey): Surface Water Temperature and Density, Pacific  
1219 Coast North and South America & Pacific Ocean Islands. U.S. Government Printing Of-  
1220 fice, Rockville, Maryland, 1967.
- 1221 USGS (United States Geological Survey): Willamette River Bathymetric Survey --  
1222 Willamette River Water Temperature Investigation. Retrieved July 28, 2022.  
1223 [https://or.water.usgs.gov/projs\\_dir/will\\_tmdl/main\\_stem\\_bth.html](https://or.water.usgs.gov/projs_dir/will_tmdl/main_stem_bth.html), 2003.
- 1224 Voelkel J. , Hellman D., Sakuma R., and Shandas V.: Assessing Vulnerability to Urban Heat: A  
1225 Study of Disproportionate Heat Exposure and Access to Refuge by Socio-Demographic  
1226 Status in Portland, Oregon. *International Journal of Environmental Research and Public  
1227 Health*, DOI: 10.3390/ijerph15040640, 2018.
- 1228 Wagner, R. W, Stacey, M.T., Brown, L.R. and Dettinger. M.: Statistical models of temperature  
1229 in the Sacramento-San Joaquin delta under climate-change scenarios and ecological im-  
1230 plications. *Estuaries and Coasts*. 34: 544-556, [https://doi.org/10.1007/s12237-010-9369-](https://doi.org/10.1007/s12237-010-9369-z)  
1231 [z](https://doi.org/10.1007/s12237-010-9369-z), 2011.
- 1232 Wallick, J.R., Grant, G., Lancaster, S., Bolte, J.P. and Denlinger, R.: Patterns and controls on  
1233 historical channel change in the Willamette River, Oregon USA. *Large Rivers: Geomor-  
1234 phology and Management*, Second Edition, pp.737-775, 2022.
- 1235 Webb B.W. and Walling D.E.: Temporal variability in the impact of river regulation on thermal  
1236 regime and some biological implications. *Freshwater Biology*, 29, 167–182,  
1237 doi.org/10.1111/j.1365-2427.1993.tb00752.x 1993.
- 1238 Webb, B. W., Clack, P.D., and Walling, D.E.: Water-air temperature relationships in a Devon  
1239 river system and the role of flow. *Hydrological Processes*. 17: 3069-3084,  
1240 <https://doi.org/10.1002/hyp.1280>, 2003.
- 1241 Webb, B. W. and Nobilis, F.: Long-term changes in river temperature and the influence of cli-  
1242 matic and hydrological factors. *Hydrological Sciences Journal*. 52(1): 74-85,  
1243 doi.org/10.1623/hysj.52.1.74, 2007.
- 1244 Weber, C., Nilsson, C., Lind, L., Alfredsen, K. T., and Polvi, L. E.: Winter disturbances and riv-  
1245 erine fish in temperate and cold regions. *BioScience*, 63(3), 199-210,  
1246 doi.org/10.1525/bio.2013.63.3.8, 2013.
- 1247 White, S.M., Justice, C. Kelsey, D.A. ,McCullough, D.A. and Smith, T.: Legacies of stream  
1248 channel modification revealed using General land Office surveys, with implications for  
1249 water temperature and aquatic life. *Elementals: Science of the Anthropocene* 5(3).  
1250 <https://doi.org/10.1525/elementa.192>, 2017.
- 1251 Willingham, W.F.: *Army Engineers and the Development of Oregon*. United States Army Corps  
1252 of Engineers, Portland, 259 pp, 1983.
- 1253 Zhu, S, Nyarko, E.K., and Hadzima-Nyarko, M.: Modelling daily water temperature from air  
1254 temperature for the Missouri River. *PeerJ*. 2018 Jun 7;6:e4894. doi: 10.7717/peerj.4894,  
1255 2018.